

Published in final edited form as:

*J Med Chem.* 2008 August 14; 51(15): 4392–4403. doi:10.1021/jm800136b.

## Optimization of the Central Heterocycle of $\alpha$ -Ketoheterocycle Inhibitors of Fatty Acid Amide Hydrolase

Joie Garfunkle, Cyrine Ezzili, Thomas J. Rayl, Dustin G. Hochstatter, Inkyu Hwang, and Dale L. Boger\*

*Department of Chemistry and The Skaggs Institute for Chemical Biology, The Scripps Research Institute, 10550 North Torrey Pines Road, La Jolla, California 92037*

### Abstract

The synthesis and evaluation of a refined series of  $\alpha$ -ketoheterocycles based on the oxazole **2** (OL-135) incorporating systematic changes in the central heterocycle bearing a key set of added substituents are described. The nature of the central heterocycle, even within the systematic and minor perturbations explored herein, significantly influenced the inhibitor activity: 1,3,4-oxadiazoles and 1,2,4-oxadiazoles **9** > tetrazoles, the isomeric 1,2,4-oxadiazoles **10**, 1,3,4-thiadiazoles > oxazoles including **2** > 1,2-diazines > thiazoles > 1,3,4-triazoles. Most evident in these trends is the observation that introduction of an additional heteroatom at position 4 (oxazole numbering, N > O > CH) substantially increases activity that may be attributed to a reduced destabilizing steric interaction at the FAAH active site. Added heterocycle substituents displaying well defined trends may be utilized to enhance the inhibitor potency and, more significantly, to enhance the inhibitor selectivity. These trends, exemplified herein, emerge from both enhancements in the FAAH activity and simultaneous disruption of binding affinity for competitive off-target enzymes.

Fatty acid amide hydrolase (FAAH)<sup>1,2</sup> is the enzyme that serves to hydrolyze endogenous lipid amides<sup>3–6</sup> including anandamide (**1a**)<sup>7–10</sup> and oleamide (**1b**),<sup>11–13</sup> Figure 1. Its distribution is consistent with its role in degrading and regulating such neuromodulating and signaling fatty acid amides at their sites of action.<sup>3</sup> Although it is a member of the amidase signature family of serine hydrolases, for which there are a number of prokaryotic enzymes, it is currently the only characterized mammalian enzyme bearing the family's unusual Ser–Ser–Lys catalytic triad.<sup>1,2,14–17</sup>

Due to the therapeutic potential of inhibiting FAAH<sup>3,18–20</sup> especially for the treatment of pain,<sup>21–23</sup> inflammatory,<sup>24</sup> or sleep disorders,<sup>13,25</sup> there has been an increasing interest in the development of selective and potent inhibitors of the enzyme.<sup>26</sup> Early studies shortly following the initial characterization of the enzyme led to the discovery that the endogenous sleep-inducing molecule 2-octyl  $\alpha$ -bromoacetoacetate is an effective FAAH inhibitor,<sup>27</sup> the disclosure of a series of nonselective reversible inhibitors bearing an electrophilic ketone (e.g., trifluoromethyl ketone-based inhibitors),<sup>28–31</sup> and the reports of a set of irreversible inhibitors<sup>32–37</sup> (e.g., fluorophosphonates and sulfonyl fluorides). To date, only two classes of inhibitors have been disclosed that provide opportunities for the development of inhibitors with therapeutic potential. One class is the reactive aryl carbamates and ureas<sup>38–50</sup> that irreversibly acylate a FAAH active site serine<sup>49</sup> and that have been shown to exhibit anxiolytic activity<sup>38</sup> and produce analgesic effects.<sup>39</sup> To date and with some exceptions, the selectivity of such inhibitors has often been low<sup>31,42,48–50</sup> further complicating the development of inhibitors that irreversibly and covalently modify the target enzyme. A second class is the  $\alpha$ -

\*Corresponding author. Phone: 858-784-7522. Fax: 858-784-7550. E-mail: boger@scripps.edu.

ketoheterocycle-based inhibitors<sup>51–59</sup> that bind to FAAH via reversible hemiketal formation with an active site serine. Many of these competitive inhibitors are not only potent and extraordinarily selective for FAAH versus other mammalian serine hydrolases, but members of this class have been shown to be efficacious analgesics in vivo.<sup>58,59</sup>

In these studies, **2**<sup>53</sup> emerged as an important lead inhibitor for further study (Figure 2). It has been shown that **2** is a potent ( $K_i = 4.7$  nM)<sup>53</sup> and selective ( $\geq 100$ –300 fold)<sup>31</sup> FAAH inhibitor that induces analgesia and increases endogenous anandamide levels.<sup>53,59</sup> It has been shown to exhibit analgesic activity in the tail flick assay, hot plate assay, formalin test of noxious chemical pain (1<sup>st</sup> and 2<sup>nd</sup> phase), the mild thermal injury (MTI) model of peripheral pain, and the spinal nerve ligation (SNL) model of neuropathic pain with efficacies that match or exceed those of morphine (@ 1–3 mg/kg in MTI/SNL), ibuprofen (@ 100 mg/kg in MTI), or gabapentin (@ 500 mg/kg in SNL) and at administered doses (10–20 mg/kg, i.p.) that approach or exceed those of such common pain medications.<sup>59</sup> It has been shown to lack significant offsite target activity (Cerep assay profiling), does not bind cannabinoid (CB1 or CB2) or vanilloid (TRP) receptors, and does not significantly inhibit common P450 metabolism enzymes (3A4, 2C9, 2D6) or the human ether-a-go-go related gene (hERG). Significantly, the inhibitor was ineffective at promoting analgesia in FAAH knockout mice<sup>58,59</sup> verifying that FAAH is the only relevant target responsible for the in vivo analgesic effects of **2**. Moreover, the analgesic effects were observed without the respiratory depression or chronic dosing desensitization characteristic of opioid administration<sup>59</sup> or the increased feeding and decreased mobility and motor control characteristic of a cannabinoid (CB1) agonist administration.<sup>59</sup>

Consequently, we conducted a series of systematic structure–activity relationship (SAR) studies on **2** independently targeting the 5-position of the central oxazole (aryl and nonaromatic substituents)<sup>53,55,56</sup> and the C2 acyl side chain,<sup>53,57,58</sup> both of which have provided extraordinarily potent and selective FAAH inhibitors (Figure 2).<sup>60</sup> Herein, we report results of systematic studies examining candidate inhibitors exploring and further optimizing the central heterocycle of the  $\alpha$ -ketoheterocycle within the structure of **2** along with results of the proteome-wide selectivity screening<sup>31</sup> of the resulting candidate inhibitors.

## Chemistry

The preparation of the 1,3,4-thiadiazole (**12**), 1,3,4-oxadiazole (**8**), and 1,2,4-oxadiazole (**9**) inhibitors is illustrated in Scheme 1. A one pot procedure was utilized to prepare the C-5 aryl substituted 1,3,4-thiadiazole, 1,3,4-oxadiazole, and 1,2,4-oxadiazole methyl esters. In the case of the 1,3,4-thiadiazole and 1,3,4-oxadiazole, the corresponding aryl(R) methyl ester was converted to the hydrazide with hydrazine monohydrate, whereas the aryl(R) nitrile was transformed to the *N*-hydroxycarbamide with hydroxylamine for the 1,2,4-oxadiazole, all of which were subsequently treated with methyl oxalyl chloride in the presence of Et<sub>3</sub>N to give a diacyl hydrazide intermediate. These were cyclized upon treatment with Lawesson's reagent to give the desired 1,3,4-thiadiazole or with *p*-toluenesulfonyl chloride (TsCl) for the 1,3,4-oxadiazole and 1,2,4-oxadiazole. Subsequent addition of the requisite side chain (**R**<sup>1</sup>) to the methyl ester was accomplished via a metal–halogen exchange of the corresponding alkylbromide to give the  $\alpha$ -ketooxadiazole or  $\alpha$ -ketothiadiazole.

Synthesis of the 1,2,4-triazole series (**14**) in an analogous fashion was unsuccessful in which the side chain nucleophilic addition to the corresponding methyl ester failed to afford product. Therefore, an alternative approach was utilized to obtain the desired 1,2,4-triazoles (Scheme 2). 7-Phenylheptanal was converted to the silyl-protected cyanohydrin upon treatment with potassium cyanide, TBSCl, and catalytic ZnI<sub>2</sub>.<sup>61</sup> The corresponding amidrazone<sup>62</sup> was formed by in situ generation of sodium hydrazine followed by dropwise addition of the cyanohydrin, which was treated with an aryl(R) acid chloride. Surprisingly, the cyclization

afforded mainly the 1,3,4-oxadiazole product along with a small amount of the desired 1,2,4-triazole product. Although this offered an additional route to the 1,3,4-oxadiazoles, it required modification for 1,2,4-triazole formation. The alternative was a two-step condensation and oxidation pathway via reaction of the amidrazone with aryl(R) aldehydes to give a stable imine, which undergoes oxidative cyclization to the triazole upon treatment with DDQ.<sup>63</sup> The desired 1,2,4-triazoles **14** were obtained after TBS deprotection (Bu<sub>4</sub>NF) and oxidation of the liberated alcohol with Dess–Martin periodinane<sup>64</sup> (Scheme 2).

The TBS protected cyanohydrin was also a key intermediate for the preparation of two additional inhibitor series, the isomeric 1,2,4-oxadiazoles (**10**) and tetrazoles (**15**). For the 1,2,4-oxadiazoles, the cyanohydrin was converted to the N-hydroxycarbamide upon treatment with hydroxylamine. Its treatment with acid chlorides in the presence of Et<sub>3</sub>N to give the diacyl hydrazide intermediates followed by dehydration with *p*-toluenesulfonyl chloride (TsCl) at elevated temperatures gave the desired 1,2,4-oxadiazoles **10** after TBS deprotection (Bu<sub>4</sub>NF) and oxidation of the liberated alcohol with Dess–Martin periodinane<sup>64</sup> (Scheme 3).

The tetrazoles (**15**) were obtained by treatment of the cyanohydrin with sodium azide.<sup>65</sup> Reprotection of the alcohol with TBSCl followed by regioselective *N*-arylation using a copper-catalyzed Ullmann condensation<sup>66</sup> with iodopyridine or with mixed-aryl hypervalent iodonium salts<sup>67</sup> afforded N2 substituted tetrazoles, which were converted to the corresponding products upon TBS deprotection (Bu<sub>4</sub>NF) and oxidation of the liberated alcohol with Dess–Martin periodinane<sup>64</sup> (Scheme 4).

The synthesis of the 1,3-thiazole inhibitors (**11**) entailed a selective C2-lithiation of thiazole followed by condensation with 7-phenylheptanal. TBS protection of the resulting alcohol followed by selective C5-lithiation (*t*-BuLi)<sup>68</sup> and stannylation or iodination and subsequent Stille coupling<sup>69</sup> produced the substituted thiazoles, which were converted to the corresponding ketones by TBS deprotection (Bu<sub>4</sub>NF) and oxidation of the liberated alcohol with Dess–Martin periodinane<sup>64</sup> (Scheme 5).

Synthesis of the 1,2-diazine inhibitors (**13**) began with Stille coupling of a known chloropyridazine<sup>70</sup> and a series of 2-(tributylstannyl)arenes or 2-aryl boronic esters to afford the series of 6-aryl substituted pyridazine-3-carboxylates. The corresponding methyl ester was converted to the aldehyde by a reduction–oxidation process in order to increase the electrophilicity of the intermediate for subsequent side chain addition, which was accomplished via metal–halogen exchange of the corresponding alkylbromide. The alcohol precursor was oxidized with Dess–Martin periodinane<sup>64</sup> to give the 1,2,-diazines **13** (Scheme 6).

## Enzyme Assay

Enzyme assays were performed at 20–23 °C with purified recombinant rat FAAH expressed in *Escherichia coli*<sup>71</sup> (unless indicated otherwise) or with solubilized COS-7 membrane extracts from cells transiently transfected with human FAAH cDNA<sup>2</sup> (where specifically indicated) in a buffer of 125 mM Tris/1 mM EDTA/0.2% glycerol/0.02% Triton X-100/0.4 mM Hepes, pH 9.0. The initial rates of hydrolysis (≤10–20% reaction) were monitored using enzyme concentrations (typically 1 nM) at least 3 times below the measured *K<sub>i</sub>* by following the breakdown of <sup>14</sup>C-oleamide, and *K<sub>i</sub>* values (standard deviations are provided in the Supporting Information tables) were established as described (Dixon plot). Lineweaver–Burk analysis previously established reversible, competitive inhibition for **2** and related inhibitors.

53

## Results and Discussion

In the course of early studies,<sup>51</sup> a range of oleyl  $\alpha$ -ketoheterocycles were explored in which the benzoxazoly<sup>51</sup> and oxazoly<sup>53</sup> derivatives were found to be among the most potent and were chosen for further examination. Their examination, which included the elaboration to the exceptionally potent oxazolopyridines<sup>51</sup> or 5-(2-pyridyl)oxazoles<sup>53</sup> including **2** defined important features of the heterocycle substituents and the C2-aryl side chain that enhance inhibitor potency or inhibitor selectivity.<sup>51–58</sup> With this knowledge of the generalized SAR surrounding these two classes of  $\alpha$ -ketoheterocycles and with the benefit of insightful modeling and computational studies<sup>72a</sup> indicating that the active site hydrogen bonding and steric interactions favor a 5-membered versus 6-membered heterocycle, we reexamined the central heterocycle extending the series to include systems not yet explored.

### Oleyl-based Inhibitors

Even before a systematic examination of the central heterocycle of **2** was undertaken, a small series of additional substituted heterocycles bearing an oleyl acyl side chain were examined beyond those originally disclosed.<sup>53</sup> This included the candidate 1,3,4-oxadiazole and 1,3,4-thiadiazole inhibitors **4a–4e** and **5a–5c**, respectively, bearing C5 substituents that probe a well-defined trend reflecting the hydrogen bond acceptor capabilities of the substituent (Figure 3). This provided inhibitors that followed the identical substituent trends ( $K_i$  for 2-pyr < 2-furyl < 2-thienyl < H) and that exhibited potencies that exceeded (**4a–4e**, 1,3,4-oxadiazoles, 2–10 fold) or roughly matched (**5a–5c**, 1,3,4-thiadiazoles) those of the corresponding oxazole (**3a–3e**).<sup>53</sup> Thus, the introduction of an additional heteroatom into the central heterocycle had a beneficial impact that in the case of the 1,3,4-oxadiazole could be attributed to a reduced destabilizing steric interaction in the active site (position 4 N vs CH) and a lower torsional energy penalty for near coplanar binding of the central heterocycle and its C5 substituent.<sup>72a</sup> These, and related studies,<sup>54</sup> indicated that systematic modifications to the central oxazole of **2** would be productive.

### Phenhexyl-based Inhibitors

The first of the inhibitors examined was the oxazole isomer **6**. Simply switching the location of the oxazole nitrogen atom within **6** resulted in a >4000-fold loss of FAAH inhibition (Figure 4). This result was anticipated based on the reduced electrophilicity of such ketones, and additional members of this class were not examined.

Much more interesting was the behavior observed in the systematic examination of alternative 5-membered heterocycles bearing two or more heteroatoms. In these comparisons, a constant series of representative C5 substituents was examined that permitted an assessment of not only the central heterocycle trends, but also served to generalize the substituent trends defined with the oxazole series.<sup>53,56</sup> In principle and because the substituent trends remain analogous across each of the heterocycles, this matrix examination confidently permits the relative extrapolation of the extensive SAR surrounding **2** and the oxazole-based inhibitors onto each of the new  $\alpha$ -ketoheterocycles (Figure 5).

Thus, the substituent impact within each heterocycle series was found to follow the well defined potency order of 2-pyr > 2-furanyl > 2-thienyl > phenyl reflecting their relative hydrogen bonding ability<sup>53</sup> and for which the 2-pyr derivatives were 10–20 fold more active than the corresponding phenyl derivative. Moreover, the unsubstituted derivative (R = H) was always less potent than the corresponding 2-pyr derivative, but more potent than the corresponding phenyl derivative displaying a  $K_i$  that approached or exceeded those of the 2-furanyl or 2-thienyl derivative. Typically, the 2-pyr-6-CO<sub>2</sub>Me derivative was less potent than the corresponding 2-pyr derivative and the corresponding 2-pyr-6-CO<sub>2</sub>H derivative was 2–10 fold

less potent than its ester. However, the results with these latter carboxylic acid derivatives represent  $K_i$ 's measured at pH 9 under conditions where they are fully ionized destabilizing their active site binding. These  $K_i$ 's improve when measured at pH 8 and 7.4 (physiological pH); for example oxazole **7g** was examined and displayed an increase in inhibitory potency with decreasing pH (**7g**: pH = 9,  $K_i$  = 20 nM; pH = 8,  $K_i$  = 14.5 nM; pH = 7.4,  $K_i$  = 10.3 nM). These overall substituent trends are analogous to those defined with the oxazole-based inhibitors (**7** series)<sup>53–58</sup> that includes **2**.

The trends for the heterocycles themselves proved even more interesting. The thiazole-based inhibitors **11** proved significantly less active than the oxazole-based inhibitors **7**, and replacing the position 4 CH of the oxazole or thiazole with a heteroatom uniformly and substantially improved the potency. The most potent of these were the 1,3,4-oxadiazoles **8** and 1,2,4-oxadiazoles **9**, which were typically 10–70 fold more active than the corresponding oxazoles, followed closely by the isomeric 1,2,4-oxadiazoles **10**. Perhaps the most dramatic change in potency occurred between the thiazole **11** and 1,3,4-thiadiazole **12** series where incorporation of the position 4 nitrogen improved potencies 30–600 fold. As such, the 1,3,4-thiadiazoles **12** typically exceed the potency of the corresponding oxazoles **7** approaching the activity of the 1,2,4-oxadiazoles **10**, albeit still being less potent than the isomeric 1,2,4-oxadiazoles **9** or 1,3,4-oxadiazoles **8**. Notably, this position 4 heteroatom effect (N > O > CH) is consistent with its role in reducing a destabilizing steric interaction at the active site as well as lowering the torsional energy penalty for coplanar binding of the heterocycle and its aryl C5 substituent.<sup>72</sup> Given that this latter effect is not contributing to the differences observed with the heterocycles when R = H, the result suggests that it is the former steric effect or an as yet unrecognized effect that dominates the differences in binding affinity. Such unrecognized effects could include the introduction of a stabilizing hydrogen bond acceptor site (N > O >> CH), heteroatom effects leading to increases in the heterocycle  $pK_b$  and intrinsic hydrogen bonding capabilities, or even simply productive increases in the intrinsic electron-withdrawing character of the central heterocycle.

Interestingly, the isosteric replacement of sulfur in the 1,3,4-thiadiazoles **12** with CH=CH, providing the corresponding 1,2-diazines **13**, afforded effective but significantly less potent inhibitors (typically 5–50 fold). Nonetheless, such inhibitors were still more effective than the corresponding triazoles **14**. The 1,2,4-triazoles **14** proved inactive, but this behavior represents the destabilizing binding of the deprotonated acidic heterocycle under the pH 9 assay conditions resulting from the C2 acyl substitution. (Figure 6).

One of the most interesting series to emerge from these studies was the tetrazoles **15**. In addition to being the most electron-deficient of the heterocycles examined, position 4 (oxazole numbering) incorporates a N (N > O > CH), and all three accessible sites on the heterocycle constitute potential hydrogen bond acceptor sites (N). Consistent with these features, the tetrazoles **15** proved substantially more active than the oxazoles **7**, comparable in potency with the 1,2,4-oxadiazoles **10**, albeit not quite as potent as the isomeric 1,2,4-oxadiazoles **9** or 1,3,4-oxadiazoles **8**. Clearly, there are subtle and unrecognized effects that account for the small differences in binding affinity between the most potent classes of heterocycles (**8**, **9** > **10**, **12**, **15**) that in turn are easily distinguished from the less active series (**13** > **11** > **14**). These latter studies with the tetrazoles seems to suggest that the most potent activity within the 5-membered heterocycles is observed with those that incorporate a hydrogen bonding acceptor N and O (vs N and N) bracketing the electrophilic carbonyl attachment site. This may account for the subtly more potent activity of the 1,3,4-oxadiazoles **8** and 1,2,4-oxadiazoles **9** (N and O) relative to the isomeric 1,2,4-oxadiazoles **10** and the comparable tetrazoles **15** (N and N). Each incorporate a heteroatom at the oxazole position 4 that enhance their activity relative to the oxazole series and the results with the tetrazole series **15** suggest the subtle differences in the **7**–**15** series has more to do with the location of the oxygen atom than a preference for an added nitrogen versus



oxygen at the oxazole position 4. The exception to the behavior in the tetrazole series **15** is the unsubstituted derivative **15a**. This unsubstituted and acidic central heterocycle, like the 1,2,4-triazole series **14**, is deprotonated under the pH 9 assay conditions destabilizing active site binding or its activation of the reversible hemiketal formation with the otherwise electrophilic carbonyl. However, simple methylation of **15a** rendered the isomeric 2- and 1-methyltetrazole derivatives **19a** and **19b**, respectively, incapable of this deprotonation and which now displayed FAAH inhibition at levels consistent with this series (Figure 6). Notably, the isomer assignments for **16–19** were made by HMBC (long range proton-carbon correlation) NMR analysis.

An additional smaller series was examined in which a methyl ester substituent was placed directly on the heterocycle (Figure 7). Such candidate FAAH inhibitors in the oxazole-based series typically display activity reflecting the strength of the conjugated electron-withdrawing substituent,<sup>55,58</sup> but lack the intrinsic enzyme selectivity observed with **2** and related inhibitors.<sup>58</sup> With the exception of the acidic triazole **14h** which was inactive presumably because of its deprotonation under the assay conditions, this substitution with **8h**, **10h**, and **12h** provided potent FAAH inhibitors ( $K_i < 10$  nM). However and unlike the behavior of the corresponding oxazole,<sup>56</sup> in each case the activity approached, but did not exceed that of the unsubstituted heterocycles (**8a**, **10a**, and **12a**).

A final series of inhibitors incorporating a substituted pyridine substituent on the central heterocycle was examined and constituted potential synthetic intermediates en route to **8f–13f** (Figure 8). Each displayed activity that approached the unsubstituted pyridine derivative (**b** series in Figure 5) or, in the case of **24** and **26**, the corresponding methyl esters **9f** and **13f**.

### Biphenylethyl-based Inhibitors

After having established that several central heterocycle replacements further improve on the potency of the oxazole-based inhibitors and that its trends in the substituent effects carry forward onto these additional  $\alpha$ -ketoheterocycles, we sought to establish that analogous modifications or substitutions in the C2 acyl side chain would be possible. Thus, a small preliminary series of key 1,3,4-oxadiazoles bearing the conformationally restricted biphenylethyl side chain was prepared (Scheme 7) and examined (Figure 9). Analogous to trends observed in the oxazole-based series,<sup>58</sup> the replacement of the phenhexyl side chain with the biphenylethyl side chain maintained or further enhanced the extraordinary potency of the candidate inhibitors (e.g.,  $K_i$  of **27** = 300 pM). Such studies continue and will be disclosed in due course.

### The Electrophilic Carbonyl

A select set of the candidate inhibitors were also examined which bear a secondary alcohol or a methylene in place of the ketone. The former were often prepared en route to the  $\alpha$ -ketoheterocycles and simply entailed examination of this alcohol intermediate. The candidate 1,3,4-oxadiazole inhibitors bearing a methylene were prepared by simple dehydrative ring closure of the corresponding diacylhydrazide as the key step (Scheme 8). Consistent with a mechanism of reversible Ser addition to the electrophilic carbonyl forming a hemiketal at the enzyme active site, the corresponding alcohol and methylene inhibitors were found to be  $\geq 10000$ -fold less active than the corresponding ketone, Figure 10. Although not investigated in detail for the inhibitors disclosed herein, even this level of reduced inhibition (0.01% activity) is most likely attributable to contaminant ketone in the samples of the alcohol and methylene compounds that can arise from air oxidation upon storage or even while undergoing the assay.<sup>56</sup> Important in these comparisons is the fact that the ketone is essential to the potent activity of the inhibitors and that reduction to an alcohol or removal altogether leads to  $\geq 10^4$  reductions in activity.

The results of an additional and unique series that were prepared (Scheme 9) and examined are summarized in Figure 11. These constitute ketone inhibitors with a methylene inserted between the reactive carbonyl and heterocycle in efforts to establish whether the inductive electron-withdrawing properties of the electron-deficient heterocycle would be sufficient to activate the carbonyl for active site hemiketal formation. Unlike the potent activity of the  $\alpha$ -ketoheterocycles, these  $\beta$ -ketoheterocycles and their corresponding alcohols were found to be inactive against FAAH.

### Inhibition of Recombinant Human FAAH

Rat and human FAAH are very homologous (82% sequence identity),<sup>2</sup> exhibit near identical substrate selectivity and inhibitor sensitivity in our studies disclosed to date, and embody an identical amidase signature sequence, suggesting the observations made with rat FAAH would be analogous to those made with the human enzyme. Consequently, key inhibitors in the series were examined against the human enzyme and were found to exhibit the same relative and absolute potencies consistent with previous observations (Figure 12).

### Selectivity

Early assessments of  $\alpha$ -ketoheterocycle inhibitors of FAAH against possible competitive enzymes (e.g., phospholipase A2, ceramidase) revealed no inhibition. Consequently, a method for proteome-wide screening capable of globally profiling all mammalian serine hydrolases was developed,<sup>31,73</sup> and studies have shown that the  $\alpha$ -ketoheterocycle class of inhibitors can be exquisitely selective for FAAH. However, two enzymes did emerge as potential competitive targets: triacylglycerol hydrolase (TGH) and a previously uncharacterized membrane-associated hydrolase that lacked known substrates or function (KIAA1363).<sup>74</sup> In this screen, IC<sub>50</sub> values are typically higher than the measured  $K_i$  values, but the relative potency, the magnitude of binding affinity differences, and the rank order binding determined in the assay parallel those established by standard substrate assays.

Summarized in Figure 13 are the results of the selectivity screening of selected candidate inhibitors. In general, the inhibitors were selective for FAAH over TGH and KIAA1363. The trends within the series examined are very clear and mirror the observations disclosed in our preceding studies.<sup>53,54,56–58</sup> Thus, the inhibitors bearing the unsubstituted heterocycles (**7–13a**) were selective for FAAH over KIAA1363, but were typically more selective for TGH over FAAH (1–125-fold). The potent inhibitors incorporating even the small methyl ester substituent (**7–12h** series) on the heterocycle were found to be selective for FAAH versus KIAA1363 (>100-fold), and now modestly selective for FAAH versus TGH (2–200-fold). In line with prior observations, the addition of a 2-pyridyl substituent (**7–15b** series) increased not only the FAAH potency, but also FAAH selectivity such that the most potent inhibitors failed to inhibit KIAA1363 (>10<sup>4</sup>-fold selective) and are now typically 4–300-fold selective for FAAH versus TGH. Addition of a C6-carboxylic acid to the 2-pyridyl substituent (**7–15g** series) further enhanced this intrinsic selectivity such that the resulting inhibitors are typically no longer viable competitive inhibitors of KIAA1363 or TGH (Figure 13 and 14). Notably, many of the central heterocycle features and added substituents that were found to increase FAAH potency were also found to enhance FAAH selectivity by simultaneously disrupting KIAA1363 and TGH affinity.

### Conclusions

Herein, we report the synthesis and evaluation of a key series of  $\alpha$ -ketoheterocycles based on **2** incorporating systematic changes in the central heterocycle that provided extraordinarily potent ( $K_i$  = 300 pM) inhibitors of fatty acid amide hydrolase. The nature of the central heterocycle, even with the modest and systematic perturbations explored herein, significantly

influenced the inhibitor activity that can be defined as 1,3,4-oxadiazoles (50) and 1,2,4-oxadiazoles **9** (50) > tetrazoles (5), the isomeric 1,2,4-oxadiazoles **10** (7), 1,3,4-thiadiazoles (2–30) > oxazoles including **2** (rel. activity = 1) > 1,2-diazines (0.3) > thiazoles (0.06) > 1,3,4-triazoles (–). Most evident in the observations is that the introduction of an additional position 4 heteroatom (oxazole numbering) substantially increases the activity (N > O > CH) that may be attributed in part to a reduced destabilizing steric interaction at the FAAH active site. Additionally the position 1 and 3 requisite heteroatoms exhibit a N,O > N,N > N,S preference that is reflected in the observed heterocycle trends. Within each heterocycle series, the impact of an added substituent was systematically explored and was found to follow well defined trends first observed with **2**. Exemplifying these effects, additional aryl substituents (e.g., 2-pyr or 2-pyr-6-CO<sub>2</sub>H) placed on the central heterocycle increase FAAH potency, and significantly modify physical properties (e.g., solubility) in a manner that may impact PK and PD behavior of the inhibitors. Just as significantly, the nature of the substituent substantially impacts the selectivity of the FAAH inhibitors and these trends proved general across the range of inhibitors examined to date.<sup>53–58</sup> This is especially evident with the TGH selectivity for the unsubstituted heterocycles (**7–13a** series, 1–100-fold selective for TGH vs FAAH) which can be improved by the independent choice of the C2 side chain (compare **2**)<sup>58</sup> as well as the heterocycle substituent (compare **7–13a** vs **7–15b** and **7–15g**). A combination of these independent features which simultaneously improve FAAH potency and disrupt TGH or KIAA1363 binding provide exquisitely selective and potent FAAH inhibitors.

## Experimental Section

### 7-Phenyl-1-(2-(pyridin-2-yl)-2H-tetrazol-5-yl)-heptan-1-one (**15b**)

A solution of 7-phenylheptanal (1.93 g, 0.01 mol) in MeCN (64 mL) was treated with KCN (2.65 g, 0.04 mol), ZnI<sub>2</sub> (77.7 mg, 0.0002 mol), and TBSCl (3.06 g, 0.02 mol) under Ar at room temperature. The reaction mixture was stirred vigorously and the progress monitored by TLC (SiO<sub>2</sub>, 5 % EtOAc–hexanes). After 72 h, the solvent was removed in vacuo and the residue resuspended in Et<sub>2</sub>O. The salts were removed by filtration and rinsed thoroughly with Et<sub>2</sub>O. The filtrate was washed with water, dried over Na<sub>2</sub>SO<sub>4</sub>, and concentrated in vacuo to give a yellow oil that was purified by flash chromatography (SiO<sub>2</sub>, 4 × 25 cm, 1% EtOAc–hexanes) to afford 2-(*tert*-butyldimethylsilyloxy)-8-phenyloctamide (2.6 g, 80%) as a colorless oil: <sup>1</sup>H NMR (CDCl<sub>3</sub>, 500 MHz) δ 7.30 (m, 2H), 7.20 (m, 3H), 4.43 (t, 1H, *J* = 6.4 Hz), 2.63 (t, 2H, *J* = 7.7 Hz), 1.80 (m, 2H), 1.65 (m, 2H), 1.49 (m, 2H), 1.39 (m, 4H), 0.94 (s, 9H), 0.21 (s, 3H), 0.16 (s, 3H); <sup>13</sup>C NMR (CDCl<sub>3</sub>, 125 MHz) δ 142.7, 128.5, 128.4, 125.7, 120.2, 62.0, 36.4, 36.0, 31.4, 29.1, 28.9, 25.6, 24.6, 18.2 (3C), –5.0, –5.2; HRMS-ESI-TOF *m/z* 354.2221 ([M + Na]<sup>+</sup>, C<sub>20</sub>H<sub>33</sub>NOSi requires 354.2223).

A sample of 2-(*tert*-butyldimethylsilyloxy)-8-phenyloctamide (335 mg, 1.01 mmol) was dissolved in a mixture of 2-propanol (1.4 mL):water (2.9 mL). NaN<sub>3</sub> (197 mg, 3.04 mmol) and ZnBr (250 mg, 1.11 mmol) were added to the reaction mixture as solids, which was subsequently warmed at 100 °C for 90 h. Upon disappearance of starting material, the solution was cooled to room temperature and diluted with EtOAc. 2 N HCl was added to the reaction mixture, which was stirred until all solids dissolved. The organic layer was isolated and the aqueous layer was washed several times with EtOAc. The combined organic phases were dried over Na<sub>2</sub>SO<sub>4</sub> and the solvent was removed under reduced pressure to afford 7-phenyl-1-(2H-tetrazol-5-yl)-heptan-1-ol as a colorless oil that was used without further purification (270 mg, quant.): <sup>1</sup>H NMR (CDCl<sub>3</sub>, 600 MHz) δ 7.25 (m, 2H), 7.15 (m, 3H), 5.26 (m, 1H), 2.57 (t, 2H, *J* = 7.7 Hz), 2.02 (m, 1H), 1.90 (m, 1H), 1.59 (m, 2H), 1.44 (m, 2H), 1.34 (m, 4H); HRMS-ESI-TOF *m/z* 261.1707 ([M + H]<sup>+</sup>, C<sub>14</sub>H<sub>20</sub>N<sub>4</sub>O requires 261.1710).

A solution of 7-phenyl-1-(2H-tetrazol-5-yl)-heptan-1-ol (36 mg, 0.14 mmol), TBSCl (63 mg, 0.42 mmol) and imidazole (28 mg, 0.42 mmol) in DMF (0.7 mL) was stirred at room



temperature for 72 h before it was diluted with EtOAc, and washed with H<sub>2</sub>O and saturated aqueous NaCl. The organic layer was dried over Na<sub>2</sub>SO<sub>4</sub> and the solvent was removed under reduced pressure to afford the crude material that was purified by flash chromatography (SiO<sub>2</sub>, 1.5 × 15 cm, 10% acetone–hexanes) to afford 5-(1-(*tert*-butyldimethylsilyloxy)-7-phenylheptyl)-2*H*-tetrazole (39 mg, 75%) as a colorless oil: <sup>1</sup>H NMR (CDCl<sub>3</sub>, 400 MHz) δ 7.26 (dd, 2H, *J* = 6.3, 8.4 Hz), 7.16 (m, 3H), 5.25 (t, 1H, *J* = 5.8 Hz), 2.57 (t, 2H, *J* = 7.7 Hz), 1.85 (m, 2H), 1.58 (m, 2H), 1.31 (m, 6H), 0.90 (s, 9H), 0.13 (s, 3H), 0.01 (s, 3H).

In a gas tight vessel, a solution of 5-(1-(*tert*-butyldimethylsilyloxy)-7-phenylheptyl)-2*H*-tetrazole (16 mg, 0.043 mmol), 2-iodopyridine (7 μL, 0.064 mmol), CuI (1 mg, 0.004 mmol), K<sub>2</sub>CO<sub>3</sub> (12 mg, 0.085 mmol), and *N,N*-dimethylethylene diamine (1 μL, 0.006 mmol) in DMF (200 μL) was purged with Ar and sealed. The reaction mixture was warmed at 100 °C for 18 h before it was cooled to room temperature, diluted with EtOAc, and washed with H<sub>2</sub>O, 9:1 NH<sub>4</sub>OH:saturated aqueous NH<sub>4</sub>Cl, and saturated aqueous NaCl. The organic layer was dried over Na<sub>2</sub>SO<sub>4</sub> and the solvent was removed under reduced pressure to afford the crude material that was purified by flash chromatography (SiO<sub>2</sub>, 1.5 × 15 cm, 5–10% acetone–hexanes) to afford 2-(5-(1-(*tert*-butyldimethylsilyloxy)-7-phenylheptyl)-2*H*-tetrazol-2-yl)-pyridine (4.0 mg, 21%) as a colorless oil: <sup>1</sup>H NMR (CDCl<sub>3</sub>, 400 MHz) δ 8.69 (dd, 1H, *J* = 0.9, 4.8 Hz), 8.16 (d, 1H, *J* = 7.5 Hz), 7.98 (dt, 1H, *J* = 1.8, 7.9 Hz), 7.48 (m, 1H), 7.26 (m, 2H), 7.16 (m, 3H), 5.16 (dd, 1H, *J* = 5.9, 7.4 Hz), 2.58 (t, 2H, *J* = 7.7 Hz), 1.99 (m, 2H), 1.60 (m, 2H), 1.34 (m, 6H), 0.88 (s, 9H), 0.10 (s, 3H), −0.02 (s, 3H); <sup>13</sup>C NMR (CDCl<sub>3</sub>, 150 MHz) δ 169.7, 149.6, 149.0, 142.9, 139.5, 128.5, 128.4, 125.7, 125.0, 115.2, 67.4, 37.5, 36.1, 31.5, 29.3, 25.9 (3C), 25.4, 18.4, −4.1, −4.8; HRMS-ESI-TOF *m/z* 452.2823 ([M+H]<sup>+</sup>, C<sub>25</sub>H<sub>37</sub>N<sub>5</sub>OSi requires 452.2840).

2-(5-(1-(*tert*-Butyldimethylsilyloxy)-7-phenylheptyl)-2*H*-tetrazol-2-yl)-pyridine (4.4 mg, 0.009 mmol) was dissolved in THF (122 μL), treated with Bu<sub>4</sub>NF (1 M in THF, 0.013 mL, 0.013 mmol) and stirred at room temperature for 2 h under Ar. The reaction mixture was diluted with EtOAc, washed with saturated aqueous NaCl and dried over Na<sub>2</sub>SO<sub>4</sub>. Evaporation in vacuo yielded the crude alcohol that was purified by flash chromatography (SiO<sub>2</sub>, 0.5 × 4 cm, 20–50% EtOAc–hexanes) to afford 7-phenyl-1-(2-(pyridin-2-yl)-2*H*-tetrazol-5-yl)-heptan-1-ol (2.7 mg, 79%) as a white solid: <sup>1</sup>H NMR (CDCl<sub>3</sub>, 600 MHz) δ 8.69 (dd, 1H, *J* = 1.1, 4.7 Hz), 8.18 (d, 1H, *J* = 8.1 Hz), 8.00 (m, 1H), 7.50 (ddd, 1H, *J* = 0.7, 4.8, 7.4 Hz), 7.26 (m, 2H), 7.16 (m, 3H), 5.16 (m, 1H), 2.59 (t, 2H, *J* = 7.7 Hz), 2.48 (d, 1H (−OH), *J* = 6.1 Hz), 2.07 (m, 2H), 1.61 (m, 2H), 1.52 (m, 2H), 1.40 (m, 4H); <sup>13</sup>C NMR (CDCl<sub>3</sub>, 150 MHz) δ 169.5, 149.6, 148.8, 142.9, 139.6, 128.5, 128.4, 125.7, 125.3, 115.3, 67.0, 36.7, 36.1, 31.5, 29.3 (2C), 25.2; HRMS-ESI-TOF *m/z* 338.1966 ([M+H]<sup>+</sup>, C<sub>19</sub>H<sub>23</sub>N<sub>5</sub>O requires 338.1975).

7-Phenyl-1-(2-(pyridin-2-yl)-2*H*-tetrazol-5-yl)-heptan-1-ol (2.7 mg, 0.007 mmol) was dissolved in CH<sub>2</sub>Cl<sub>2</sub> (0.24 mL) and Dess–Martin periodinane (4.5 mg, 0.011 mmol) was added. The mixture was stirred at room temperature for 2 h before the reaction mixture was reduced to half volume and this mixture was directly loaded onto silica gel and purified by flash chromatography (SiO<sub>2</sub>, 0.5 × 4 cm, 10–30% EtOAc–hexanes) to afford 7-phenyl-1-(2-(pyridin-2-yl)-2*H*-tetrazol-5-yl)-heptan-1-one (**15b**, 2.7 mg, 99%) as a white solid: <sup>1</sup>H NMR (CDCl<sub>3</sub>, 600 MHz) δ 8.74 (m, 1H), 8.23 (m, 1H), 8.05 (dt, 1H, *J* = 1.6, 7.9 Hz), 7.57 (dd, 1H, *J* = 4.8, 7.5 Hz), 7.27 (t, 2H, *J* = 7.6 Hz), 7.17 (m, 3H), 3.26 (t, 2H, *J* = 7.4 Hz), 2.61 (t, 2H, *J* = 7.7 Hz), 1.83 (m, 2H), 1.64 (m, 2H), 1.43 (m, 4H); <sup>13</sup>C NMR (CDCl<sub>3</sub>, 150 MHz) δ 191.5, 162.5, 149.9, 148.6, 142.8, 139.8, 128.5, 128.4, 126.0, 125.8, 115.9, 41.0, 36.0, 31.4, 29.1, 29.0, 23.5; HRMS-ESI-TOF *m/z* 336.1813 ([M+H]<sup>+</sup>, C<sub>19</sub>H<sub>21</sub>N<sub>5</sub>O requires 336.1819). Purity 99%.

## FAAH Inhibition

<sup>14</sup>C-labeled oleamide was prepared from <sup>14</sup>C-labeled oleic acid as described.<sup>13</sup> The truncated rat FAAH (rFAAH) was expressed in *E. coli* and purified as described.<sup>71</sup> The purified recombinant rFAAH was used in the inhibition assays unless otherwise indicated. The full-length human FAAH (hFAAH) was expressed in COS-7 cells as described,<sup>2</sup> and the lysate of hFAAH-transfected COS-7 cells was used in the inhibition assays where explicitly indicated.

The inhibition assays were performed as described.<sup>13</sup> In brief, the enzyme reaction was initiated by mixing 1 nM of rFAAH (800, 500, or 200 pM rFAAH for inhibitors with  $K_i \leq 1$ –2 nM) with 10  $\mu$ M of <sup>14</sup>C-labeled oleamide in 500  $\mu$ L of reaction buffer (125 mM TrisCl, 1 mM EDTA, 0.2% glycerol, 0.02% Triton X-100, 0.4 mM Hepes, pH 9.0) at room temperature in the presence of three different concentrations of inhibitor. The enzyme reaction was terminated by transferring 20  $\mu$ L of the reaction mixture to 500  $\mu$ L of 0.1 N HCl at three different time points. The <sup>14</sup>C-labeled oleamide (substrate) and oleic acid (product) were extracted with EtOAc and analyzed by TLC as detailed.<sup>13</sup> The  $K_i$  of the inhibitor was calculated using a Dixon plot as described (standard deviations are provided in the Supporting Information tables). Lineweaver-Burk analysis was performed as described confirming competitive, reversible inhibition.<sup>53</sup>

## Selectivity Screening

The selectivity screening was conducted as detailed.<sup>31</sup>

## Supplementary Material

Refer to Web version on PubMed Central for supplementary material.

## Acknowledgements

We gratefully acknowledge the financial support of the National Institutes of Health (DA15648) and the Skaggs Institute for Chemical Biology. We wish to acknowledge Dr. Wu Du and his preparation of **4b**, **4e**, **8b**, **8c**, **8e** (ref. 54), Dr. Robert Fecik for the preparation of **4a** and **5a**, and Dr. F. Anthony Romero for the preparation of **6**. We are especially grateful to Professor B. F. Cravatt for the supply of rat and recombinant human FAAH and to H. S. Hoover in the Cravatt laboratories for the training and guidance in conducting the selectivity assay. JG is a Skaggs and A.R.C.S. Fellow.

## References

1. Cravatt BF, Giang DK, Mayfield SP, Boger DL, Lerner RA, Gilula NB. Molecular Characterization of an Enzyme that Degrades Neuromodulatory Fatty Acid Amides. *Nature* 1996;384:83–87. [PubMed: 8900284]
2. Giang DK, Cravatt BF. Molecular Characterization of Human and Mouse Fatty Acid Amide Hydrolases. *Proc Natl Acad Sci USA* 1997;94:2238–2242. [PubMed: 9122178]
3. Patricelli MP, Cravatt BF. Proteins Regulating the Biosynthesis and Inactivation of Neuromodulatory Fatty Acid Amides. *Vit Hormones* 2001;62:95–131.
4. Egertova M, Cravatt BF, Elphick MR. Comparative Analysis of Fatty Acid Amide Hydrolase and CB1 Cannabinoid Receptor Expression in the Mouse Brain: Evidence of a Widespread Role for Fatty Acid Amide Hydrolase in Regulation of Endocannabinoid Signaling. *Neuroscience* 2003;119:481–496. [PubMed: 12770562]
5. Boger DL, Fecik RA, Patterson JE, Miyauchi H, Patricelli MP, Cravatt BF. Fatty Acid Amide Hydrolase Substrate Specificity. *Bioorg Med Chem Lett* 2000;10:2613–2616. [PubMed: 11128635]
6. Lang W, Qin C, Lin S, Khanolkar AD, Goutopoulos A, Fan P, Abouzid K, Meng Z, Biegel D, Makriyannis A. Substrate Specificity and Stereoselectivity of Rat Brain Microsomal Anandamide Amidohydrolase. *J Med Chem* 1999;42:896–902. [PubMed: 10072686]

7. Devane WA, Hanus L, Breuer A, Pertwee RG, Stevenson LA, Griffin G, Gibson D, Mandelbaum A, Etinger A, Mechoulam R. Isolation and Structure of a Brain Constituent that Binds to the Cannabinoid Receptor. *Science* 1992;258:1946–1949. [PubMed: 1470919]
8. Martin BR, Mechoulam R, Razdan RK. Discovery and Characterization of Endogenous Cannabinoids. *Life Sci* 1999;65:573–595. [PubMed: 10462059]
9. Di Marzo V, Bisogno T, De Petrocellis L, Melck D, Martin BR. Cannabimimetic Fatty Acid Derivatives: The Anandamide Family and Other “Endocannabinoids”. *Curr Med Chem* 1999;6:721–744. [PubMed: 10469888]
10. Schmid HHO, Schmid PC, Natarajan V. *N*-Acylated Glycerophospholipids and Their Derivatives. *Prog Lipid Res* 1990;29:1–43. [PubMed: 2087478]
11. Boger DL, Henriksen SJ, Cravatt BF. Oleamide: An Endogenous Sleep-Inducing Lipid and Prototypical Member of a New Class of Lipid Signaling Molecules. *Curr Pharm Des* 1998;4:303–314. [PubMed: 10197045]
12. Cravatt BF, Lerner RA, Boger DL. Structure Determination of an Endogenous Sleep-Inducing Lipid, *cis*-9-Octadecenamide (Oleamide): A Synthetic Approach to the Chemical Analysis of Trace Quantities of a Natural Product. *J Am Chem Soc* 1996;118:580–590.
13. Cravatt BF, Prospero-Garcia O, Suizdak G, Gilula NB, Henriksen SJ, Boger DL, Lerner RA. Chemical Characterization of a Family of Brain Lipids that Induce Sleep. *Science* 1995;268:1506–1509. [PubMed: 7770779]
14. Patricelli MP, Cravatt BF. Fatty Acid Amide Hydrolase Competitively Degrades Bioactive Amides and Esters Through a Nonconventional Catalytic Mechanism. *Biochemistry* 1999;38:14125–14130. [PubMed: 10571985]
15. Patricelli MP, Cravatt BF. Clarifying the Catalytic Roles of Conserved Residues in the Amidase Signature Family. *J Biol Chem* 2000;275:19177–19184. [PubMed: 10764768]
16. Patricelli MP, Lovato MA, Cravatt BF. Chemical and Mutagenic Investigations of Fatty Acid Amide Hydrolase: Evidence for a Family of Serine Hydrolases with Distinct Catalytic Properties. *Biochemistry* 1999;38:9804–9812. [PubMed: 10433686]
17. Bracey MH, Hanson MA, Masuda KR, Stevens RC, Cravatt BF. Structural Adaptations in a Membrane Enzyme that Terminates Endocannabinoid Signaling. *Science* 2002;298:1793–1796. [PubMed: 12459591]
18. Fowler CJ, Jonsson K-D, Tiger G. Fatty Acid Amide Hydrolase: Biochemistry, Pharmacology, and Therapeutic Possibilities for an Enzyme Hydrolyzing Anandamide, 2-Arachidonoylglycerol, Palmitoylethanolamide, and Oleamide. *Biochem Pharmacol* 2001;62:517–526. [PubMed: 11585048]
19. Cravatt BF, Lichtman AH. Fatty Acid Amide Hydrolase: An Emerging Therapeutic Target in the Endocannabinoid System. *Curr Opin Chem Biol* 2003;7:469–475. [PubMed: 12941421]
20. Lambert DM, Fowler CJ. The Endocannabinoid System: Drug Targets, Lead Compounds, and Potential Therapeutic Applications. *J Med Chem* 2005;48:5059–5087. [PubMed: 16078824]
21. Cravatt BF, Demarest K, Patricelli MP, Bracey MH, Giang DK, Martin BR, Lichtman AH. upersensitivity to Anandamide and Enhanced Endogenous Cannabinoid Signaling in Mice Lacking Fatty Acid Amide Hydrolase. *Proc Natl Acad Sci USA* 2001;98:9371–9376. [PubMed: 11470906]
22. Lichtman AH, Shelton CC, Advani T, Cravatt BF. Mice Lacking Fatty Acid Amide Hydrolase Exhibit a Cannabinoid Receptor-Mediated Phenotypic Hypoalgesia. *Pain* 2004;109:319–327. [PubMed: 15157693]
23. Cravatt BF, Saghatelian A, Hawkins EG, Clement AB, Bracey MH, Lichtman AH. Functional Disassociation of the Central and Peripheral Fatty Acid Amide Signaling Systems. *Proc Natl Acad Sci USA* 2004;101:10821–10826. [PubMed: 15247426]
24. Karsak M, Gaffal E, Date R, Wang-Eckhardt L, Rehnelt J, Petrosino S, Starowicz K, Steuder R, Schlicker E, Cravatt BF, Mechoulam R, Buettner R, Werner S, Di Marzo V, Tuetting T, Zimmer A. Attenuation of Allergic Contact Dermatitis Through the Endocannabinoid System. *Science* 2007;316:1494–1497. [PubMed: 17556587]
25. (a) Huitrón-Reséndiz S, Gombart L, Cravatt BF, Henriksen SJ. Effect of Oleamide on Sleep and Its Relationship to Blood Pressure, Body Temperature, and Locomotor Activity in Rats. *Exp Neurol* 2001;172:235–243. [PubMed: 11681856] (b) Huitrón-Reséndiz S, Sanchez-Alavez M, Wills DN,

- Cravatt BF, Henriksen SJ. Characterization of the Sleep-Wake Patterns in Mice Lacking Fatty Acid Amide Hydrolase. *Sleep* 2004;27:857–865. [PubMed: 15453543]
26. Clement AB, Hawkins EG, Lichtman AH, Cravatt BF. Increased Seizure Susceptibility and Proconvulsant Activity of Anandamide in Mice Lacking Fatty Acid Amide Hydrolase. *J Neurosci* 2003;23:3916–3923. [PubMed: 12736361]
  27. Patricelli MP, Patterson JP, Boger DL, Cravatt BF. An Endogenous Sleep-Inducing Compound is a Novel Competitive Inhibitor of Fatty Acid Amide Hydrolase. *Bioorg Med Chem Lett* 1998;8:613–618. [PubMed: 9871570]
  28. Koutek B, Prestwich GD, Howlett AC, Chin SA, Salehani D, Akhavan N, Deutsch DG. Inhibitors of Arachidonoyl Ethanolamide Hydrolysis. *J Biol Chem* 1994;269:22937–22940. [PubMed: 8083191]
  29. Patterson JE, Ollmann IR, Cravatt BF, Boger DL, Wong C-H, Lerner RA. Inhibition of Oleamide Hydrolase Catalyzed Hydrolysis of the Endogenous Sleep-Inducing Lipid *cis*-9-Octadecenamide. *J Am Chem Soc* 1996;118:5938–5945.
  30. Boger DL, Sato H, Lerner AE, Austin BJ, Patterson JE, Patricelli MP, Cravatt BF. trifluoromethyl Ketone Inhibitors of Fatty Acid Amide Hydrolase: A Probe of Structural and Conformational Features Contributing to Inhibition. *Bioorg Med Chem Lett* 1999;9:265–270. [PubMed: 10021942]
  31. Leung D, Hardouin C, Boger DL, Cravatt BF. Discovering Potent and Selective Reversible Inhibitors of Enzymes in Complex Proteomes. *Nature Biotech* 2003;21:687–691.
  32. De Petrocellis L, Melck D, Ueda N, Maurelli S, Kurahashi Y, Yamamoto S, Marino G, Di Marzo V. Novel Inhibitors of Brain, Neuronal, and Basophilic Anandamide Amidohydrolase. *Biochem Biophys Res Commun* 1997;231:82–88. [PubMed: 9070224]
  33. Deutsch DG, Omeir R, Arreaza G, Salehani D, Prestwich GD, Huang Z, Howlett A. Methyl Arachidonoyl Fluorophosphonate: A Potent Irreversible Inhibitor of Anandamide Amidase. *Biochem Pharmacol* 1997;53:255–260. [PubMed: 9065728]
  34. Deutsch DG, Lin S, Hill WAG, Morse KL, Salehani D, Arreaza G, Omeir RL, Makriyannis A. Fatty Acid Sulfonyl Fluorides Inhibit Anandamide Metabolism and Bind to the Cannabinoid Receptor. *Biochem Biophys Res Commun* 1997;231:217–221. [PubMed: 9070252]
  35. Edgemond WS, Greenberg MJ, McGinley PJ, Muthians S, Campbell WB, Hillard CJ. Synthesis and Characterization of Diazomethylarachidonoyl Ketone: An Irreversible Inhibitor of *N*-Arachidonyl ethanolamine Amidohydrolase. *J Pharmacol Exp Ther* 1998;286:184–190. [PubMed: 9655859]
  36. Fernando SR, Pertwee RG. Evidence that Methyl Arachidonoyl Fluorophosphonate is an Irreversible Cannabinoid Receptor Antagonist. *Br J Pharmacol* 1997;121:1716–1720. [PubMed: 9283708]
  37. Du W, Hardouin C, Cheng H, Hwang I, Boger DL. Heterocyclic Sulfoxide and Sulfone Inhibitors of Fatty Acid Amide Hydrolase. *Bioorg Med Chem Lett* 2005;15:103–106. [PubMed: 15582420]
  38. (a) Kathuria S, Gaetani S, Fegley D, Valino F, Duranti A, Tontini A, Mor M, Tarzia G, La Rana G, Calignano A, Giustino A, Tattoli M, Palmery M, Cuomo V, Piomelli D. Modulation of Anxiety Through Blockade of Anandamide Hydrolysis. *Nat Med* 2003;9:76–81. [PubMed: 12461523] (b) Gobbi G, Bambico FR, Mangieri R, Bortolato M, Campolongo P, Solinas M, Cassano T, Morgese MG, Debonnel G, Duranti A, Tontini A, Tarzia G, Mor M, Trezza V, Goldberg SR, Cuomo V, Piomelli D. Antidepressant-Like Activity and Modulation of Brain Monoaminergic Transmission by Blockage of Anandamide Hydrolase. *Proc Natl Acad Sci USA* 2005;102:18620–18625. [PubMed: 16352709]
  39. Jayamanne A, Greenwood R, Mitchell VA, Aslan S, Piomelli D, Vaughan CW. Actions of the FAAH Inhibitor URB597 in Neuropathic and Inflammatory Chronic Pain Models. *Br J Pharmacol* 2006;147:281–288. [PubMed: 16331291]
  40. Mor M, Rivara S, Lodola A, Plazzi PV, Tarzia G, Duranti A, Tontini A, Piersanti G, Kathuria S, Piomelli D. Cyclohexylcarbamic Acid 3'- or 4'-Substituted Biphenyl-3-yl Esters as Fatty Acid Amide Hydrolase Inhibitors: Synthesis, Quantitative Structure–Activity Relationships, and Molecular Modeling Studies. *J Med Chem* 2004;47:4998–5008. [PubMed: 15456244]
  41. (a) Tarzia G, Duranti A, Tontini A, Piersanti G, Mor M, Rivara S, Plazzi PV, Park C, Kathuria S, Piomelli D. Design, Synthesis, and Structure–Activity Relationships of Alkylcarbamic Acid Aryl Esters, a New Class of Fatty Acid Amide Hydrolase Inhibitors. *J Med Chem* 2003;46:2352–2360. [PubMed: 12773040] (b) Tarzia G, Duranti A, Gatti G, Piersanti G, Tontini A, Rivara S, Lodola A,

- Plazzi PV, Mor M, Kathuria S, Piomelli D. Synthesis and Structure–Activity Relationships of FAAH Inhibitors: Cyclohexylcarbamic Acid Biphenyl Esters with Chemical Modulation at the Proximal Phenyl Ring. *Chem Med Chem* 2006;1:130–139. [PubMed: 16892344]
42. Ahn K, Johnson DS, Fitzgerald LR, Liimatta M, Arendse A, Stevenson T, Lund ET, Nugent RA, Normanbhoy T, Alexander JP, Cravatt BF. A Novel Mechanistic Class of Fatty Acid Amide Hydrolase Inhibitors with Remarkable Selectivity. *Biochemistry* 2007;46:13019–13030. [PubMed: 17949010]
43. (a) Abouab–Dellah, A.; Burnier, P.; Hoornaert, C.; Jeunesse, J.; Puech, F. WO 2004/099176, Derivatives of Piperidinyl- and Piperazinyl-alkyl Carbamates, Preparation Methods and Application in Therapeutics (Sanofi). Abouab–Dellah, A.; Almario, G. A.; Froissant, J.; Hoornaert, C. WO 2005/077898, Aryloxyalkylcarbamate Derivatives, Including Piperidine Carbamates, Their Preparation and Use as Fatty Acid Amide Hydrolase (FAAH) Inhibitors for Treating FAAH-Related Pathologies (Sanofi). (c) Abouab–Dellah, A.; Almario, G. A.; Hoornaert, C.; Li, A. T. WO 2005/070910, 1-Piperazine and 1-Homopiperazine Derivatives, Their Preparation and Use as Fatty Acid Amide Hydrolase (FAAH) Inhibitors for Treating FAAH-Related Pathologies (Sanofi). (d) Abouab–Dellah, A.; Almario, G. A.; Hoornaert, C.; Li, A. T. WO 2007/027141, Alkyl(homo) piperazine-carboxylate Derivatives, Their Preparation and Use as Fatty Acid Amide Hydrolase (FAAH) Inhibitors for Treating FAAH-Related Pathologies (Sanofi).
44. Sit, S-Y.; Xie, K.; Deng, H. WO2003/06589, Preparation of (Hetero)aryl Carbamates and Oximes as Fatty Acid Amide Hydrolase Inhibitors. Bristol–Myers Squibb; Sit, S-Y.; Xie, K. WO 2002/087569, Preparation of Bis Arylimidazolyl Fatty Acid Amide Hydrolase Inhibitors for Treatment of Pain. Bristol–Myers Squibb; (c) Sit SY, Conway C, Bertekap R, Xie K, Bourin C, Burris K, Deng H. Novel Inhibitors of Fatty Acid Amide Hydrolase. *Bioorg Med Chem Lett* 2007;17:3287–3291. [PubMed: 17459705]
45. (a) Apodaca, R.; Breitenbucher, J. G.; Pattabiraman, K.; Seierstad, M.; Xiao, W. US 2006/0173184, Piperazinyl and Piperidinyl Ureas as Modulators of Fatty Acid Amide Hydrolase (J&J). (b) Apodaca, R.; Breitenbucher, J. G.; Pattabiraman, K.; Seierstad, M.; Xiao, W. US 2007/004741, Preparation of Thiadiazolylpiperazine Carboxamides as Modulators of Fatty Acid Amide Hydrolase (FAAH) (J&J).
46. (a) Matsumoto, T.; Kori, M.; Miyazaki, J.; Kiyota, Y. WO 2006054652, Preparation of Piperidinecarboxamides and Piperazinecarboxamides as Fatty Acid Amide Hydrolase (FAAH) Inhibitors (Takeda) (b) Matsumoto, T.; Kori, M.; Kouno, M. WO 2007020888, Preparation of Piperazine-1-carboxamide Derivatives as Brain/Neuronal Cell-protecting Agents, and Therapeutic Agents for Sleep Disorder (Takeda).
47. Ishii, T.; Sugane, T.; Maeda, J.; Narazaki, F.; Kakefuda, A.; Sato, K.; Takahashi, T.; Kanayama, T.; Saitoh, C.; Suzuki, J.; Kanai, C. WO 2006/088075, Preparation of Pyridyl Non-Aromatic Nitrogenated Heterocyclic-1-carboxylate Ester Derivatives as FAAH Inhibitors (Astellas).
48. (a) Moore SA, Nomikos GG, Dickason–Chesterfield AK, Sohober DA, Schaus JM, Ying BP, Xu YC, Phebus L, Simmons RM, Li D, Iyengar S, Felder CC. Identification of a High-Affinity Binding Site Involved in the Transport of Endocannabinoids (LY2183240). *Proc Natl Acad Sci USA* 2005;102:17852–17857. [PubMed: 16314570] (b) Alexander JP, Cravatt BF. The Putative Endocannabinoid Transport Blocker LY2183240 is a Potent Inhibitor of FAAH and Several Other Brain Serine Hydrolases. *J Am Chem Soc* 2006;128:9699–9704. [PubMed: 16866524]
49. Alexander JP, Cravatt BF. Mechanism of Carbamate Inactivation of FAAH: Implications for the Design of Covalent Inhibitors and In Vivo Functional Probes for Enzymes. *Chem Biol* 2005;12:1179–1187. [PubMed: 16298297]
50. Zhang D, Saraf A, Kolasa T, Bhatia P, Zheng GZ, Patel M, Lannoye GS, Richardson P, Stewart A, Rogers JC, Brioni JD, Surowy CS. Fatty Acid Amide Hydrolase Inhibitors Display Broad Selectivity and Inhibit Multiple Carboxylesterases as Off-Targets. *Neuropharmacol* 2007;52:1095–1105.
51. Boger DL, Sato H, Lerner AE, Hedrick MP, Fecik RA, Miyauchi H, Wilkie GD, Austin BJ, Patricelli MP, Cravatt BF. Exceptionally Potent Inhibitors of Fatty Acid Amide Hydrolase: The Enzyme Responsible for Degradation of Endogenous Oleamide and Anandamide. *Proc Natl Acad Sci USA* 2000;97:5044–5049. [PubMed: 10805767]
52. Boger DL, Miyauchi H, Hedrick MP.  $\alpha$ -Keto Heterocycle Inhibitors of Fatty Acid Amide Hydrolase: Carbonyl Group Modification and  $\alpha$ -Substitution. *Bioorg Med Chem Lett* 2001;11:1517–1520. [PubMed: 11412972]



53. Boger DL, Miyauchi H, Du W, Hardouin C, Fecik RA, Cheng H, Hwang I, Hedrick MP, Leung D, Acevedo O, Guimarães CRW, Jorgensen WL, Cravatt BF. Discovery of a Potent, Selective, and Efficacious Class of Reversible  $\alpha$ -Ketoheterocycle Inhibitors of Fatty Acid Amide Hydrolase as Analgesics. *J Med Chem* 2005;48:1849–1856. [PubMed: 15771430]
54. Leung D, Du W, Hardouin C, Cheng H, Hwang I, Cravatt BF, Boger DL. Discovery of an Exceptionally Potent and Selective Class of Fatty Acid Amide Hydrolase Inhibitors Enlisting Proteome-Wide Selectivity Screening: Concurrent Optimization of Enzyme Inhibitor Potency and Selectivity. *Bioorg Med Chem Lett* 2005;15:1423–1428. [PubMed: 15713400]
55. Romero FA, Hwang I, Boger DL. Delineation of a Fundamental  $\alpha$ -Ketoheterocycle Substituent Effect for Use in the Design of Enzyme Inhibitors. *J Am Chem Soc* 2006;68:14004–14005. [PubMed: 17061864]
56. Romero FA, Du W, Hwang I, Rayl TJ, Kimball FS, Leung D, Hoover HS, Apodaca RL, Breitenbucher BJ, Cravatt BF, Boger DL. Potent and Selective  $\alpha$ -Ketoheterocycle-Based Inhibitors of the Anandamide and Oleamide Catabolizing Enzyme, Fatty Acid Amide Hydrolase. *J Med Chem* 2007;50:1058–1068. [PubMed: 17279740]
57. Hardouin C, Kelso MJ, Romero FA, Rayl TJ, Leung D, Hwang I, Cravatt BF, Boger DL. Structure–Activity Relationships of  $\alpha$ -Ketooxazole Inhibitors of Fatty Acid Amide Hydrolase. *J Med Chem* 2007;50:3359–3368. [PubMed: 17559203]
58. Kimball FS, Romero FA, Ezzili C, Garfunkle J, Rayl TJ, Hochstater DG, Hwang I, Boger DL. Optimization of  $\alpha$ -Ketooxazole Inhibitors of Fatty Acid Amide Hydrolase. *J Med Chem* 2008;51:937–947. [PubMed: 18247553]
59. (a) Lichtman AH, Leung D, Shelton CC, Saghatelian A, Hardouin C, Boger DL, Cravatt BF. Reversible Inhibitors of Fatty Acid Amide Hydrolase that Promote Analgesia: Evidence for an Unprecedented Combination of Potency and Selectivity. *J Pharmacol Exp Ther* 2004;311:441–448. [PubMed: 15229230] (b) Chang L, Luo L, Palmer JA, Sutton S, Wilson SJ, Barbier AJ, Breitenbucher JG, Chaplan SR, Webb M. Inhibition of Fatty Acid Amide Hydrolase Produces Analgesia by Multiple Mechanisms. *Br J Pharmacol* 2006;148:102–113. [PubMed: 16501580]
60. For additional studies, see: (a) Muccioli GG, Fazio N, Scriba GKE, Poppitz W, Cannata F, Poupaert JH, Wouters J, Lambert DM. Substituted 2-Thioxoimidazolidin-4-ones and Imidazolidine-2,4-diones as Fatty Acid Amide Hydrolase Inhibitors Templates. *J Med Chem* 2006;49:417–425. [PubMed: 16392827] (b) Saario SM, Poso A, Juvonen RO, Jarvinen T, Salo-Ahen OMH. Fatty Acid Amide Hydrolase Inhibitors from Virtual Screening of the Endocannabinoid System. *J Med Chem* 2006;49:4650–4656. [PubMed: 16854070] (c) Myllymaki MJ, Saario SM, Kataja AO, Castillo-Melendez JA, Navalainen T, Juvonen RO, Jarvinen T, Koskinen AMP. Design, Synthesis, and In Vitro Evaluation of Carbamate Derivatives of 2-Benzoxazolyl- and 2-Benzothiazolyl-(3-hydroxyphenyl)-methanones as Novel Fatty Acid Amide Hydrolase Inhibitors. *J Med Chem* 2007;50:4236–4242. [PubMed: 17665899]
61. Rawal VH, Rao JA, Cava MP. A Convenient Synthesis of *t*-Butyldimethylsilyl Protected Cyanohydrins. *Tetrahedron Lett* 1985;26:4275–4278.
62. (a) Kauffman, Th. Reactions of Sodium Hydrazide with Organic Compounds. *Angew Chem Int Ed* 1964;3:342–353. (b) Garg NK, Stoltz BM. Synthesis of Bis(indole)-1,2,4-triazinones. *Tetrahedron Lett* 2005;46:1997–2000. (c) Li JH, Snyder JK. Pyrrole as a Dienophile in Intramolecular Inverse Electron-Demand Diels-Alder Reactions with 1,2,4-Triazines. *J Org Chem* 1993;58:516–519.
63. (a) Walker D, Hiebert JD. 2,3-Dichloro-5,6-dicyanobenzoquinone and Its Reactions. *Chem Rev* 1967;67:153–195. [PubMed: 4859921] (b) Bruché L, Zecchi G. The Intramolecular Nitrile Imine Cycloaddition Route to Pyrazolo[1,5-*a*][1,4]benzodiazepines. *Tetrahedron* 1989;45:7427–7432.
64. Dess DB, Martin JC. A Useful 12-I-5 Triacetoxyperiodinane (the Dess–Martin Periodinane) for the Selective Oxidation of Primary or Secondary Alcohols and a Variety of Related 12-I-5 Species. *J Am Chem Soc* 1991;113:7277–7287.
65. Demko ZP, Sharpless KB. An Expedient Route to the Tetrazole Analogues of  $\alpha$ -Amino Acids. *Org Lett* 2002;4:2525–2527. [PubMed: 12123367]
66. (a) Ley SV, Thomas AW. Modern Synthetic Methods for Copper-Mediated C(aryl)–O, C(aryl)–N, and C(aryl)–S Bond Formation. *Angew Chem Int Ed* 2003;42:5400–5449. (b) Christau H-J, Cellier PP, Spindler J-F, Taillefer M. Highly Efficient and Mild Copper-Catalyzed N- and C-Arylations with Aryl Bromides and Iodides. *Chem Eur J* 2004;10:5607–5622. (c) Antilla JC, Baskin JM, Barder TE,

- Buchwald SL. Copper-Diamine-Catalyzed N-Arylation of Pyrroles, Pyrazoles, Indazoles, Imidazoles, and Triazoles. *J Org Chem* 2004;69:5578–5587. [PubMed: 15307726]
67. (a) Beletskaya IP, Davydov DV, Gorovoy MS. Palladium- and Copper-Catalyzed Selective Arylation of 5-Aryltetrazoles by Diaryliodonium Salts. *Tetrahedron Lett* 2002;43:6221–6223. Davydov DV, Beletskaya IP, Semenov BB, Smushkevich YI. Regioselective Arylation of N-Tributylstannylated 5-Substituted Tetrazoles by Diaryliodonium Salts in the Presence of Cu(OAc)<sub>2</sub>. *Tetrahedron Lett* 2002;43:6217–6219. (b) Carroll MA, Pike VW, Widdowson DA. New Synthesis of Diaryliodonium Sulfonates from Arylboronic Acids. *Tetrahedron Lett* 2000;41:5393–5396.
68. Stangeland EL, Sammakia T. Use of Thiazoles in the Halogen Dance Reaction: Application to the Total Synthesis of WS75624 B. *J Org Chem* 2004;69:2381–2385. [PubMed: 15049634] For a review, see: Iddon B. Synthesis and Reactions of Lithiated Monocyclic Azoles Containing Two or More Hetero-Atoms. Part V: Isothiazoles and Thiazoles. *Heterocycles* 1995;41:533–593.
69. Farina V, Krishnamurthy V, Scott WJ. The Stille Reaction. *Org React* 1997;50:1–652.
70. Olsen AG, Dahl O, Nielsen PE. Synthesis and Evaluation of a Conformationally Constrained Pyridazinone PNA-monomer for Recognition of Thymine in Triple-helix Structures. *Bioorg Med Chem Lett* 2004;14:1551–1554. [PubMed: 15006401]
71. Patricelli MP, Lashuel HA, Giang DK, Kelly JW, Cravatt BF. Comparative Characterization of a Wild Type and Transmembrane Domain-Deleted Fatty Acid Amide Hydrolase: Identification of the Transmembrane Domain as a Site for Oligomerization. *Biochemistry* 1998;37:15177–15187. [PubMed: 9790682]
72. (a) Guimarães CRW, Boger DL, Jorgensen WL. Elucidation of Fatty Acid Amide Hydrolase Inhibition by Potent  $\alpha$ -Ketoheterocycle Derivatives from Monte Carlo Simulations. *J Am Chem Soc* 2005;127:17377–17384. [PubMed: 16332087] (b) Tubert-Brohman I, Acevedo O, Jorgensen WL. Elucidation of Hydrolysis Mechanisms for Fatty Acid Amide Hydrolase and its Lys142Ala Variant via QM/MM Simulations. *J Am Chem Soc* 2006;128:16904–16913. [PubMed: 17177441]
73. (a) Kidd D, Liu Y, Cravatt BF. Profiling Serine Hydrolase Activities in Complex Proteomes. *Biochemistry* 2001;40:4005–4015. [PubMed: 11300781] (b) Liu Y, Patricelli MP, Cravatt BF. Activity-Based Protein Profiling: the Serine Hydrolases. *Proc Natl Acad Sci USA* 1999;96:14694–14699. [PubMed: 10611275]
74. Chiang KP, Niessen S, Saghatelian A, Cravatt BF. An Enzyme that Regulates Ether Lipid Signaling Pathways in Cancer Annotated by Multidimensional Profiling. *Chem Biol* 2006;13:1041–1050. [PubMed: 17052608]

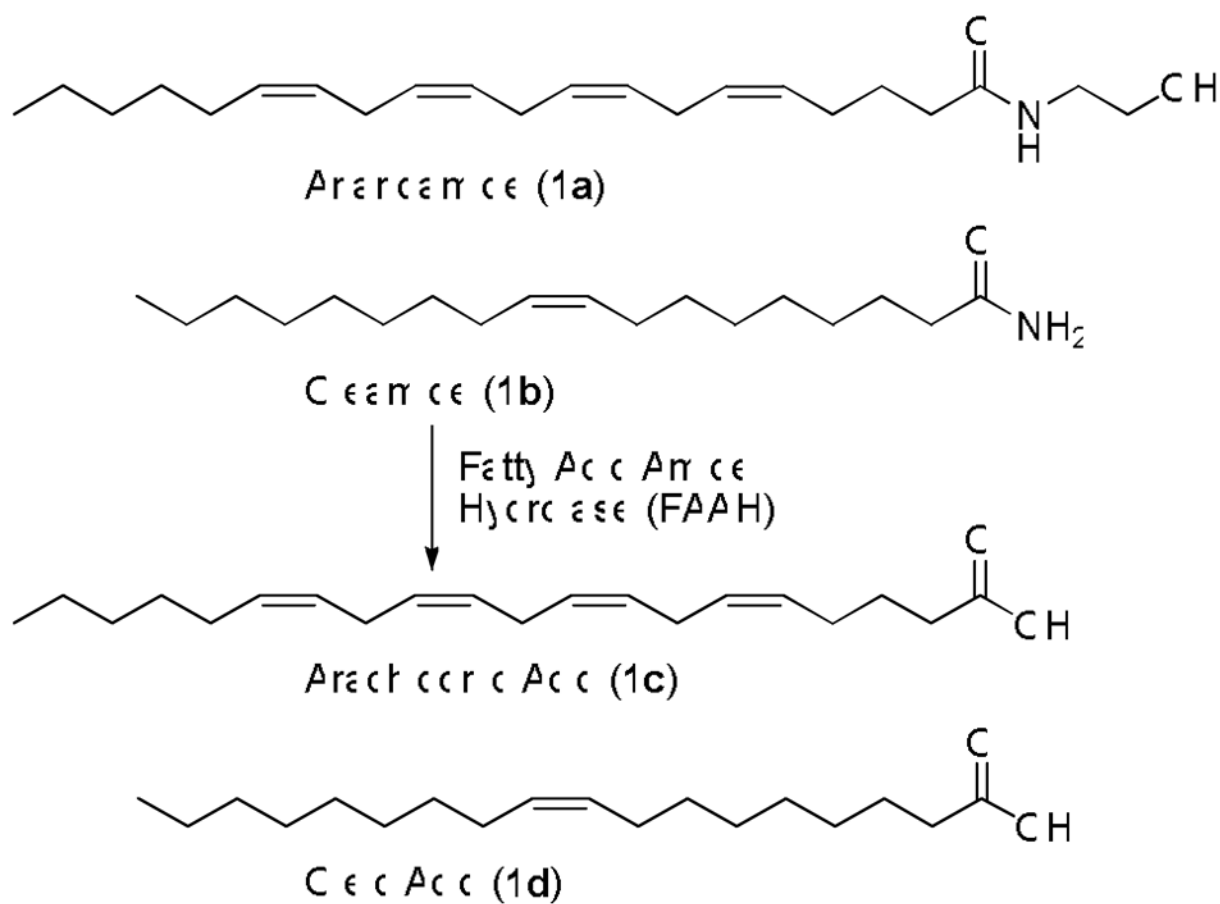
## Abbreviations

### FAAH

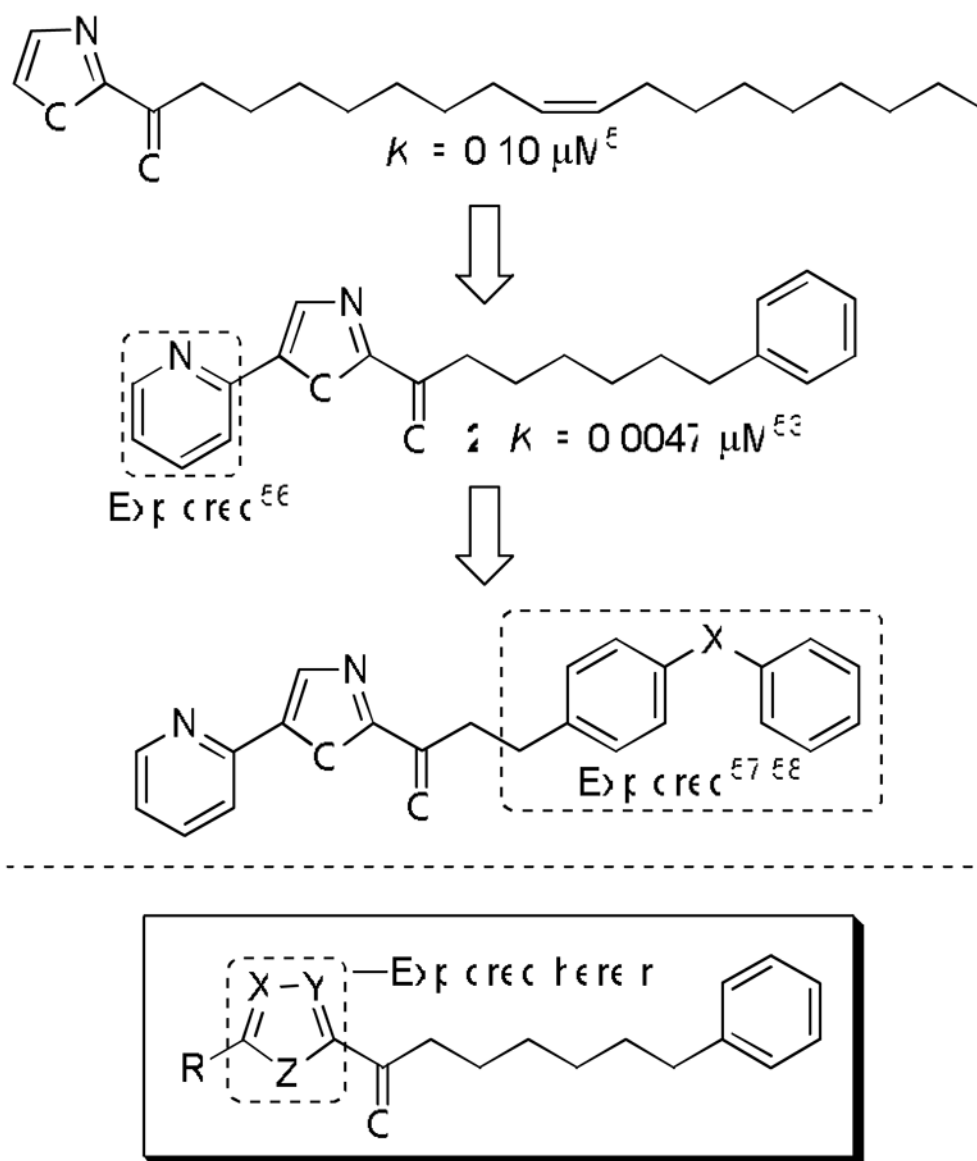
fatty acid amide hydrolase

### TGH

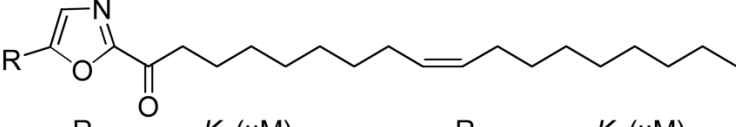
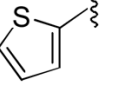
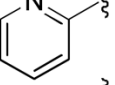
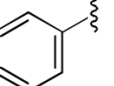
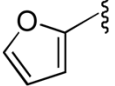
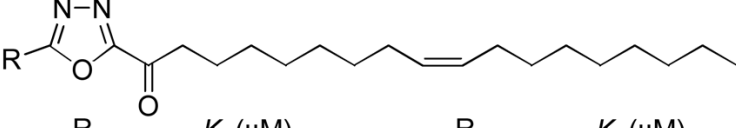
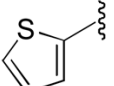
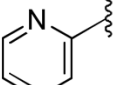
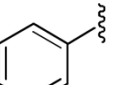
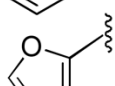
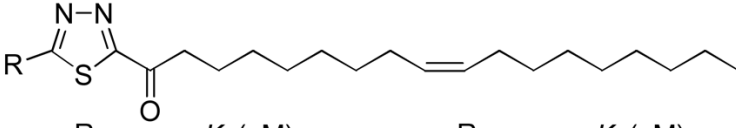
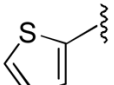
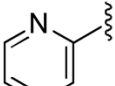
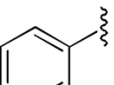
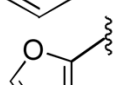
triacylglycerol hydrolase



**Figure 1.**  
Substrates of fatty acid amide hydrolase (FAAH).

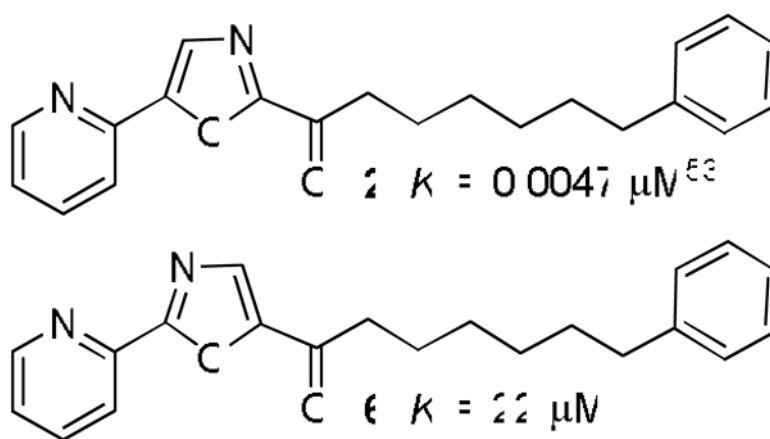


**Figure 2.**  
Progression of the inhibitor series.

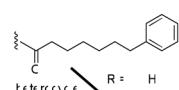
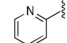
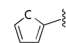
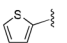
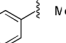
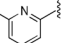
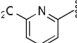
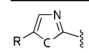
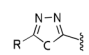
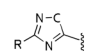
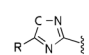
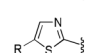
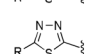
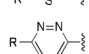
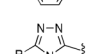
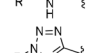
			
R	$K_i$ ( $\mu$ M)	R	$K_i$ ( $\mu$ M)
<b>3a</b> H	0.100 <sup>53</sup>	<b>3d</b> 	0.089 <sup>53</sup>
<b>3b</b> 	0.018 <sup>53</sup>	<b>3e</b> 	0.320 <sup>53</sup>
<b>3c</b> 	0.054 <sup>53</sup>		
<hr/>			
			
R	$K_i$ ( $\mu$ M)	R	$K_i$ ( $\mu$ M)
<b>4a</b> H	0.090 <sup>54</sup>	<b>4d</b> 	0.008
<b>4b</b> 	0.003 <sup>54</sup>	<b>4e</b> 	0.016 <sup>54</sup>
<b>4c</b> 	0.005		
<hr/>			
			
R	$K_i$ ( $\mu$ M)	R	$K_i$ ( $\mu$ M)
<b>5a</b> H	0.170		—
<b>5b</b> 	0.020		—
<b>5c</b> 	0.150		

**Figure 3.**  
Oleyl-based inhibitors.





**Figure 4.**  
Activity of the isomeric oxazole.

							
	R = H						
	48 (7a) <sup>2d</sup>	47 (7b) <sup>2d</sup>	12 (7c) <sup>2d</sup>	55 (7d) <sup>2d</sup>	80 (7e) <sup>2d</sup>	80 (7f) <sup>2d</sup>	20 (7g) <sup>2d</sup>
	10 (8a)	0.9 (8b) <sup>2d</sup>	0.56 (8c) <sup>2d</sup>	0.80 (8d)	22 (8e) <sup>2d</sup>	30 (8f)	14 (8g) <sup>2d</sup>
	10 (9a)	0.34 (9b)	10 (9c)	16 (9d)	—	30 (9f)	13 (9g) <sup>2d</sup>
	70 (10a)	11 (10b)	85 (10c)	44 (10d)	—	70 (10f)	53 (10g) <sup>2d</sup>
	800 (11a)	24 (11b)	1500 (11c)	2000 (11d)	—	500 (11f)	10000 (11g) <sup>2d</sup>
	14 (12a)	0.80 (12b)	74 (12c)	27 (12d)	—	77 (12f)	50 (12g) <sup>2d</sup>
	140 (13a)	25 (13b)	40 (13c)	46 (13d)	—	110 (13f)	360 (13g) <sup>2d</sup>
	>1000 (14a) <sup>2d</sup>	>100000 (14b) <sup>2d</sup>	>1000 (14c) <sup>2d</sup>	>1000 (14d) <sup>2d</sup>	—	—	—
	>1000 (15a) <sup>2d</sup>	11 (15b)	50 (15c)	85 (15d)	16 (15e)	—	—

<sup>2d</sup>Depicted at the pH = 9 assays (see text)

**Figure 5.**  
Inhibitors containing alternative central heterocycles,  $K_i$  (nM).

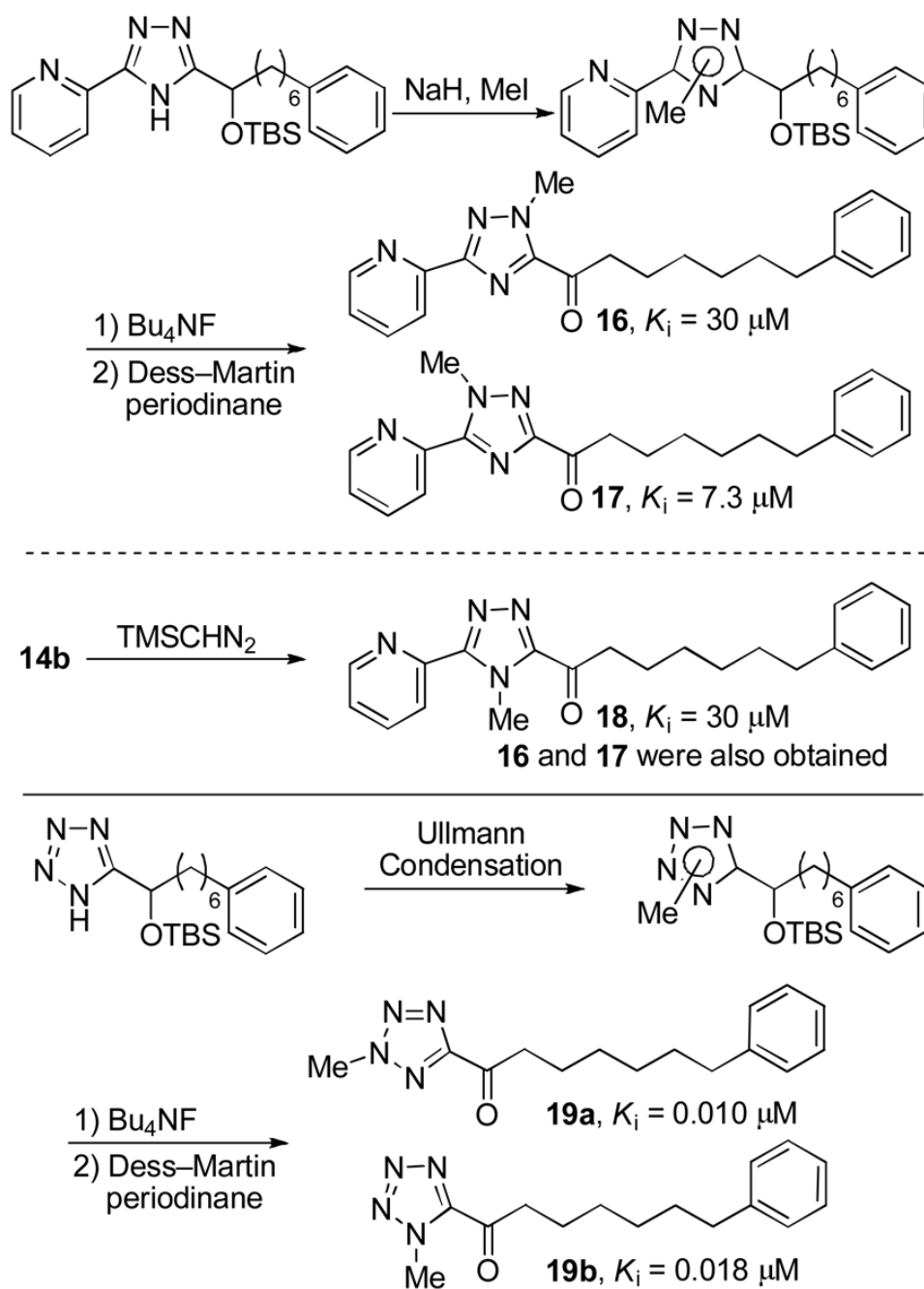


**Figure 6.**  
Effect of *N*-methylation on inhibitor potency of 1,2,4-triazoles and tetrazoles.

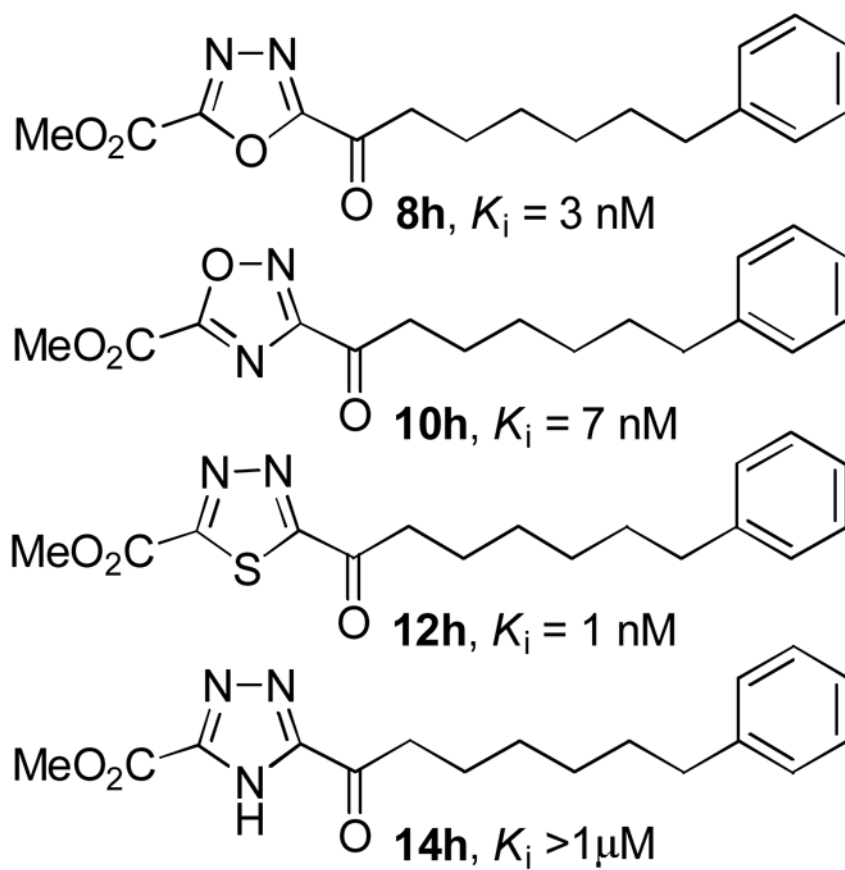


**Figure 7.**  
Methyl ester substituted  $\alpha$ -ketoheterocycle inhibitors of FAAH.

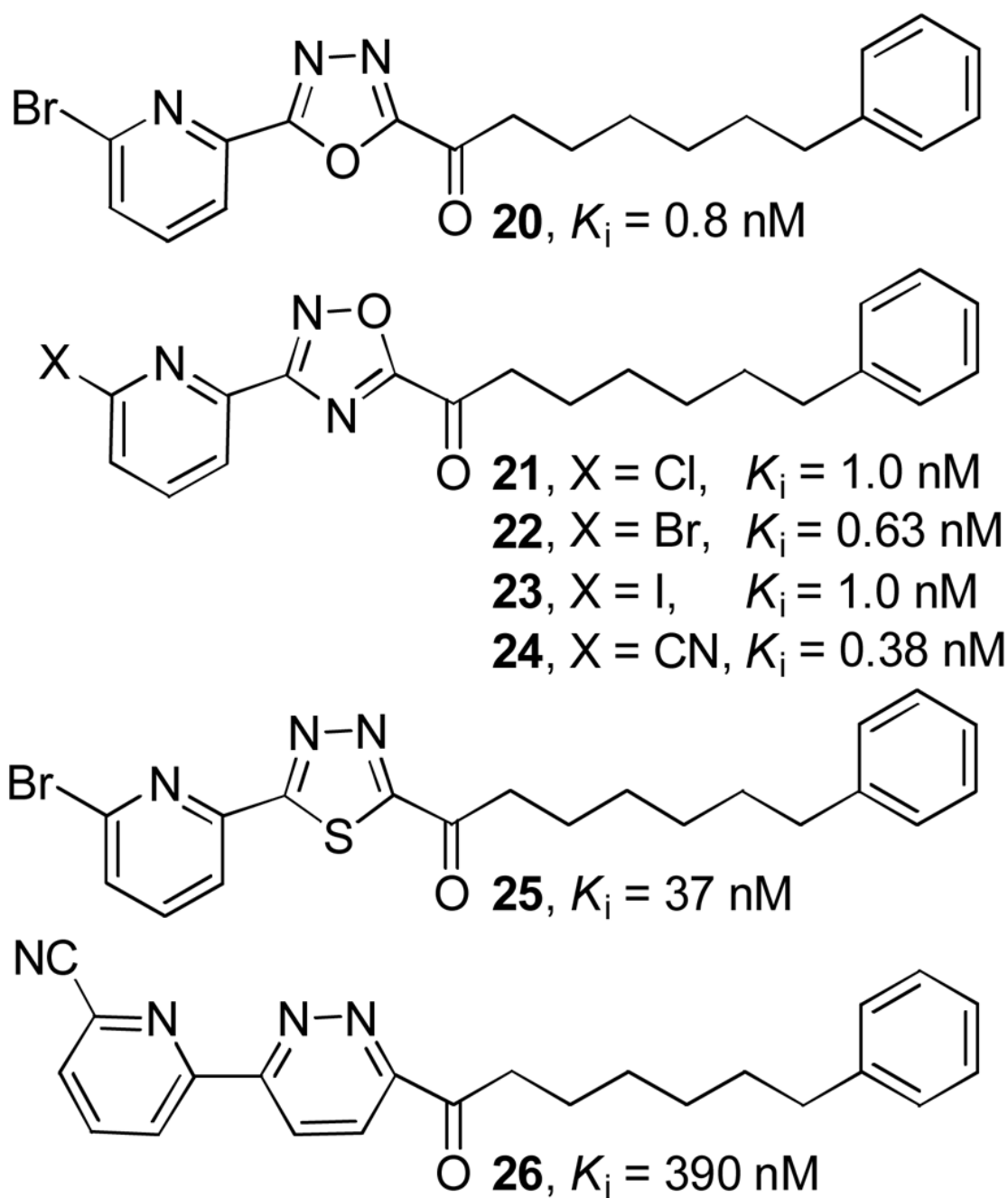


**Figure 8.**  
Additional C6 substituted 2-pyridyl substituents.



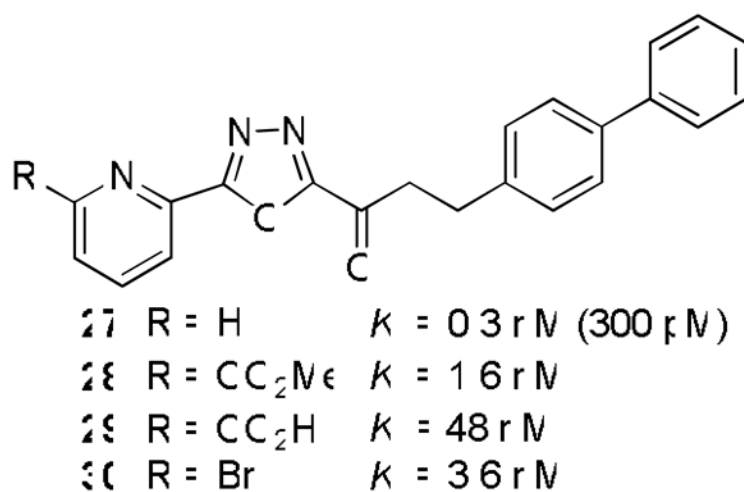
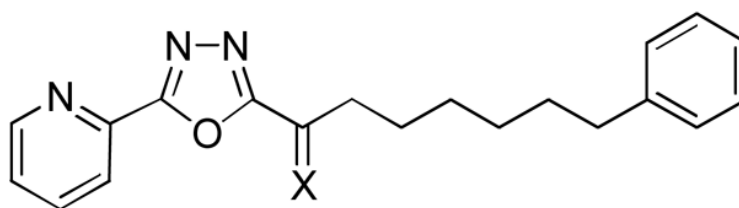
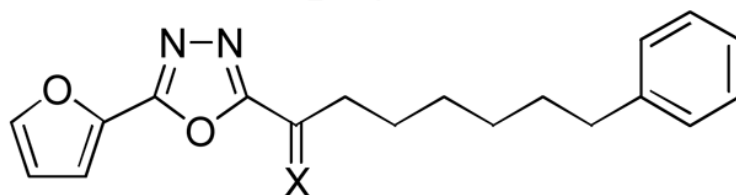


**Figure 9.**  
Biphenylethyl-based inhibitors.



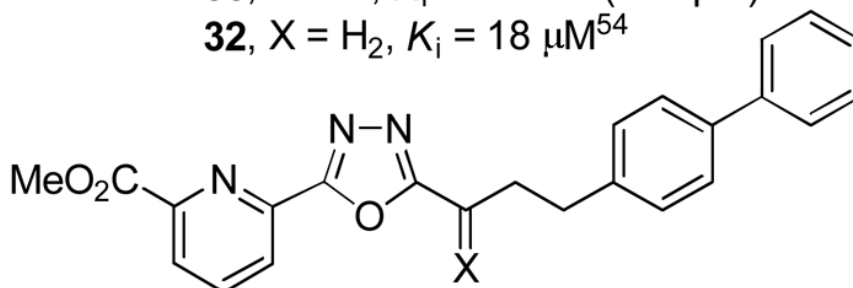
**8b**, X = O,  $K_i$  = 0.29 nM (290 pM)

**31**, X = H<sub>2</sub>,  $K_i$  = 60  $\mu$ M<sup>54</sup>



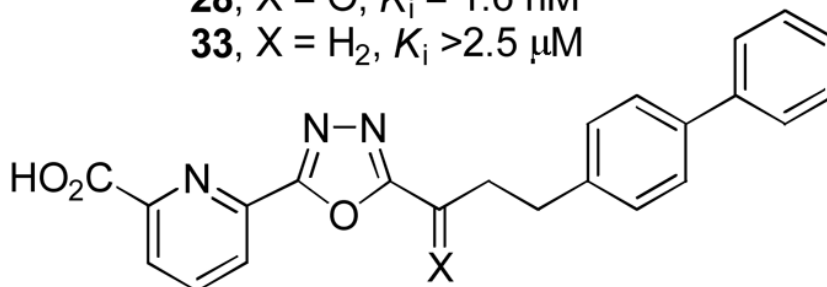
**8c**, X = O,  $K_i$  = 0.5 nM (500 pM)

**32**, X = H<sub>2</sub>,  $K_i$  = 18  $\mu$ M<sup>54</sup>



**28**, X = O,  $K_i$  = 1.6 nM

**33**, X = H<sub>2</sub>,  $K_i$  > 2.5  $\mu$ M



**29**, X = O,  $K_i$  = 48 nM

**34**, X = H<sub>2</sub>,  $K_i$  > 2.5  $\mu$ M

**Figure 10.**  
Effect of the electrophilic carbonyl.

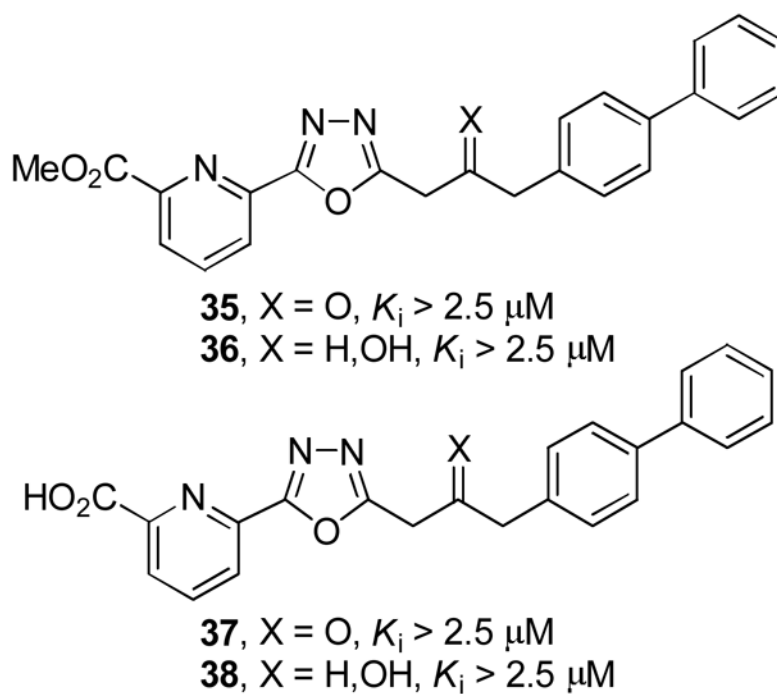


**Figure 11.**  
 $\beta$ -keto-1,3,4-oxadiazoles.

compd	$K_{\text{m}} \mu\text{M}$ (linear)	$K_{\text{m}} \mu\text{M}$ (rat)
7b	0.0090	0.0047
7g	0.026	0.020
8b	0.0012	0.00029
8g	0.037	0.014
9b	0.00092	0.00034
10b	0.016	0.0011
10g	0.110	0.053
12b	0.003	0.0008
15b	0.0055	0.0011

**Figure 12.**  
Inhibition of recombinant human fatty acid amide hydrolase.

	FAAH $K_i$ , $\mu\text{M}$	FAAH $\text{IC}_{50}$ , $\mu\text{M}$	KIAA1363 $\text{IC}_{50}$ , $\mu\text{M}$	TGH $\text{IC}_{50}$ , $\mu\text{M}$		
<b>Oxazole series</b>						
7a R = H	0.048	2.5	20 (8)	0.02 (0.008) <sup>56</sup>		
2 R = 2-pyr	0.0047	0.002	>100 (>50000)	0.6 (300) <sup>53</sup>		
7c R = 2-furanyl	0.012	0.08	>100 (>1250)	0.3 (4) <sup>53</sup>		
7d R = 2-thiophenyl	0.055	0.8	>100 (>125)	0.2 (0.25) <sup>53</sup>		
7e R = Ph	0.08	0.9	>100 (>110)	0.7 (0.8)		
7f R = 2-pyr-6-CO <sub>2</sub> Me	0.008	0.17	40 (240)	1.0 (6)		
7g R = 2-pyr-6-CO <sub>2</sub> H	0.02	0.1	>100 (>1000)	>100 (>1000) <sup>56</sup>		
7h R = CO <sub>2</sub> Me	0.0009	0.03	>100 (>3300)	0.3 (10)		
<b>1,3,4-Oxadiazole series</b>						
8a R = H	0.001	0.016	>100 (>6250)	0.025 (1.5)		
8b R = 2-pyr	0.00029	0.001	90 (90000)	0.14 (140) <sup>54</sup>		
8c R = 2-furanyl	0.00056	0.001	>100 (>10 <sup>5</sup> )	0.08 (80) <sup>54</sup>		
8e R = Ph	0.0022	0.025	>100 (>4000)	0.25 (10) <sup>54</sup>		
8f R = 2-pyr-6-CO <sub>2</sub> Me	0.003	0.008	>100 (>12500)	0.04 (5)		
8g R = 2-pyr-6-CO <sub>2</sub> H	0.014	0.1	>100 (>1000)	40 (400)		
8h R = CO <sub>2</sub> Me	0.001	1.0	>100 (>100)	2.0 (2)		
<b>1,2,4-Oxadiazole series 9</b>						
9a R = H	0.001	0.004	25 (6250)	0.0007 (0.18)		
9b R = 2-pyr	0.00034	0.003	30 (10000)	0.03 (10)		
9f R = 2-pyr-6-CO <sub>2</sub> Me	0.003	0.003	40 (13000)	0.15 (50)		
9g R = 2-pyr-6-CO <sub>2</sub> H	0.013	0.04	>100 (>2500)	40 (1000)		
<b>1,2,4-Oxadiazole series 10</b>						
10a R = H	0.007	0.5	>100 (>200)	0.01 (0.02)		
10b R = 2-pyr	0.0011	0.007	>100 (>14000)	0.4 (60)		
10f R = 2-pyr-6-CO <sub>2</sub> Me	0.007	0.3	>100 (>330)	3.0 (10)		
10g R = 2-pyr-6-CO <sub>2</sub> H	0.053	0.07	>100 (>1400)	>100 (>1400)		
10h R = CO <sub>2</sub> Me	0.007	0.01	>100 (>10000)	0.2 (20)		
<b>Thiazole series</b>						
11a R = H	0.8	>100	>100 (1)	2 (<0.02)		
11b R = 2-pyr	0.024	2	>100 (>50)	8 (4)		
11f R = 2-pyr-6-CO <sub>2</sub> Me	0.5	>100	>100 (1)	40 (<0.4)		
11g R = 2-pyr-6-CO <sub>2</sub> H	10	8	>100 (>12)	30 (4)		
<b>1,3,4-Thiadiazole series</b>						
12a R = H	0.0014	0.3	>100 (>330)	0.1 (1)		
12b R = 2-pyr	0.0008	0.03	>100 (>3300)	4.5 (150)		
12f R = 2-pyr-6-CO <sub>2</sub> Me	0.0077	0.8	>100 (>125)	0.8 (1)		
12g R = 2-pyr-6-CO <sub>2</sub> H	0.050	3	>100 (>33)	>100 (>33)		
12h R = CO <sub>2</sub> Me	0.001	0.06	>100 (>1700)	11 (180)		
<b>1,2-Diazine series</b>						
13a R = H	0.14	3	>100 (>30)	5 (1)		
13b R = 2-pyr	0.025	6	>100 (>20)	>100 (>20)		
13f R = 2-pyr-6-CO <sub>2</sub> Me	0.110	10	>100 (>10)	>100 (>10)		
13g R = 2-pyr-6-CO <sub>2</sub> H	0.360	20	>100 (>5)	>100 (>5)		
13h R = 2-pyr-6-CN	0.390	13	>100 (>8)	12 (1)		
<b>Tetrazole series</b>						
15a R = Me	0.010	0.6	60 (100)	0.08 (0.13)		
15b R = 2-pyr	0.0011	0.003	>100 (>30000)	0.12 (40)		

**Figure 13.**  
Activity based protein profiling of FAAH  $\alpha$ -ketoheterocycles.



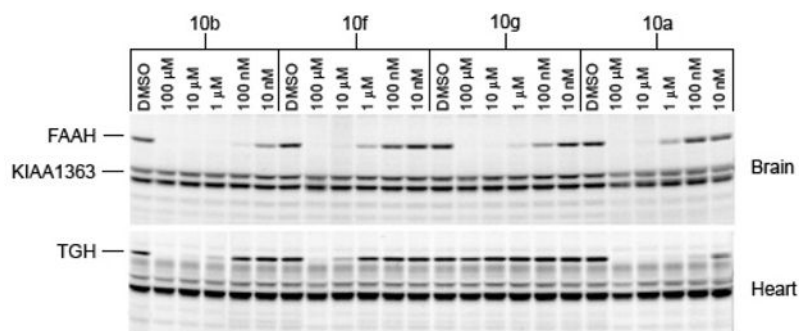
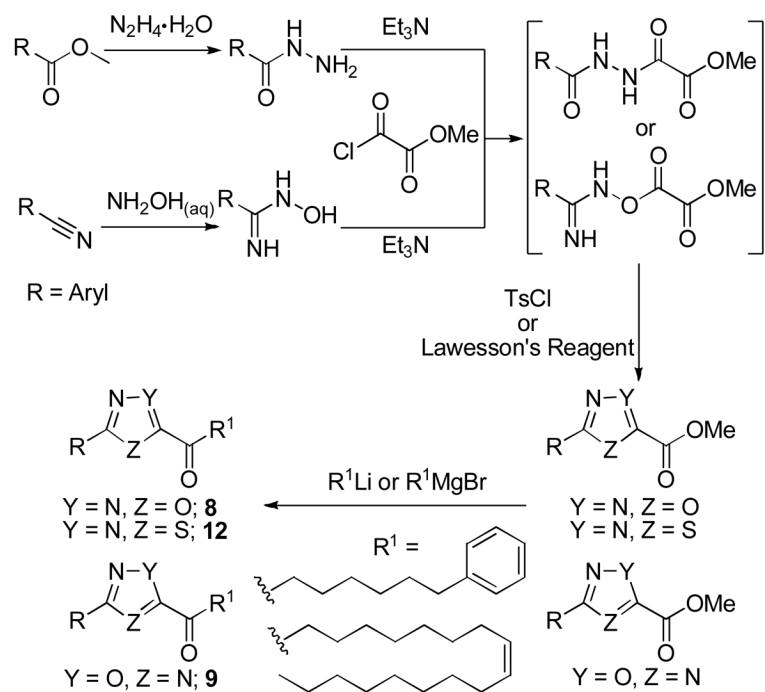
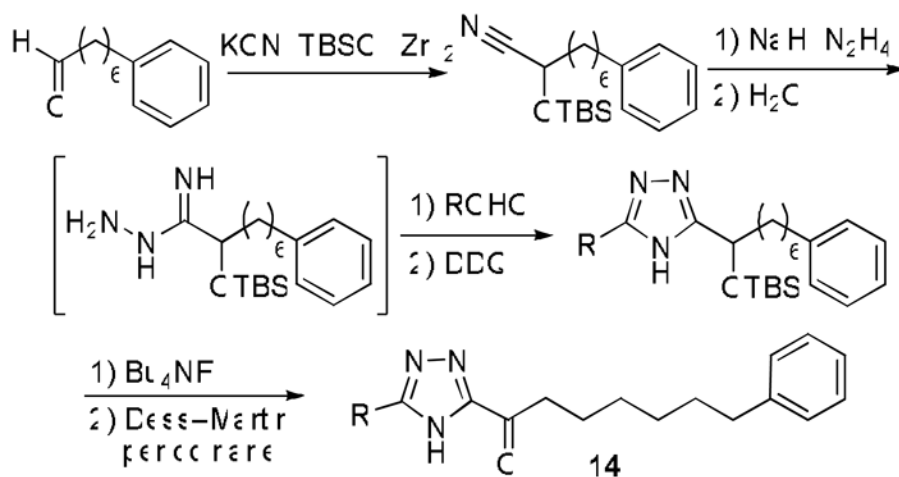


**Figure 14.**

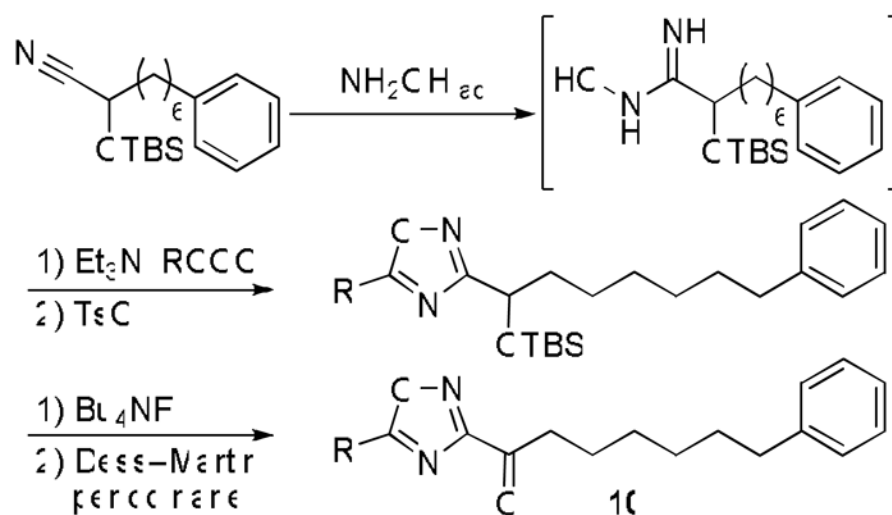
Activity based protein profiling of FAAH inhibitors **10b**, **10f**, **10g**, **10a** with FP-Rh in brain and heart membrane proteome. Enzyme targets such as FAAH, KIAA1363, and TGH are highlighted.



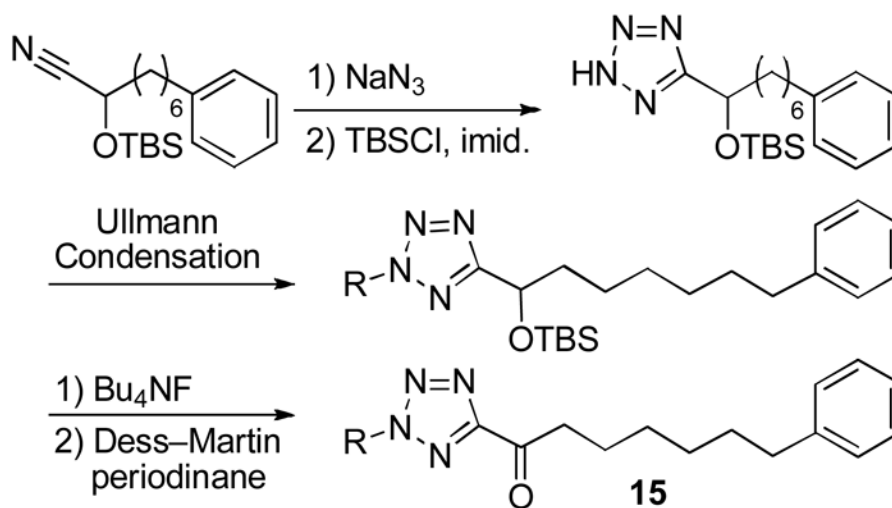
Scheme 1.



Scheme 2.

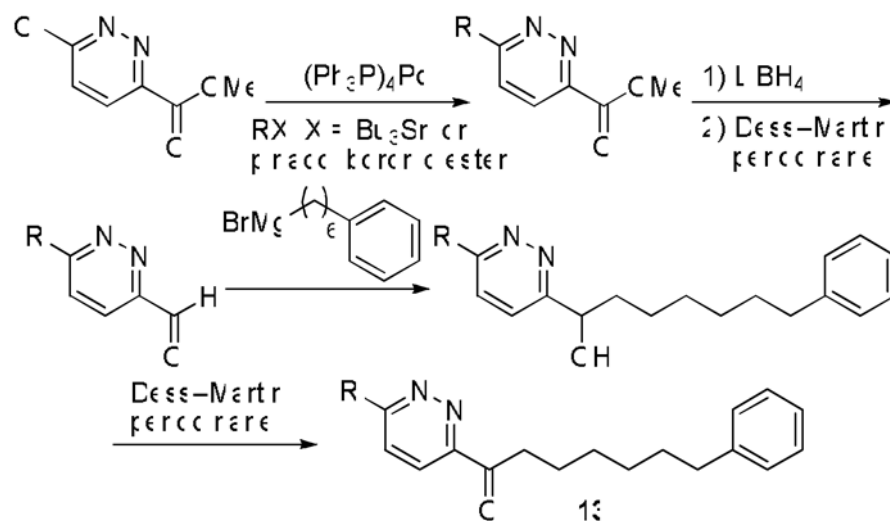


Scheme 3.



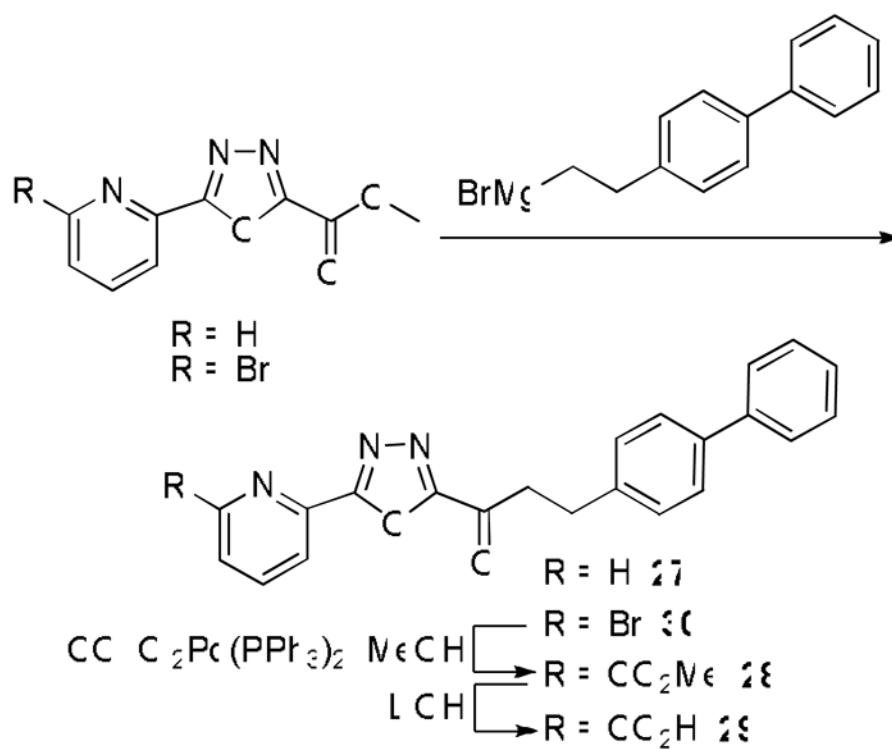
Scheme 4.



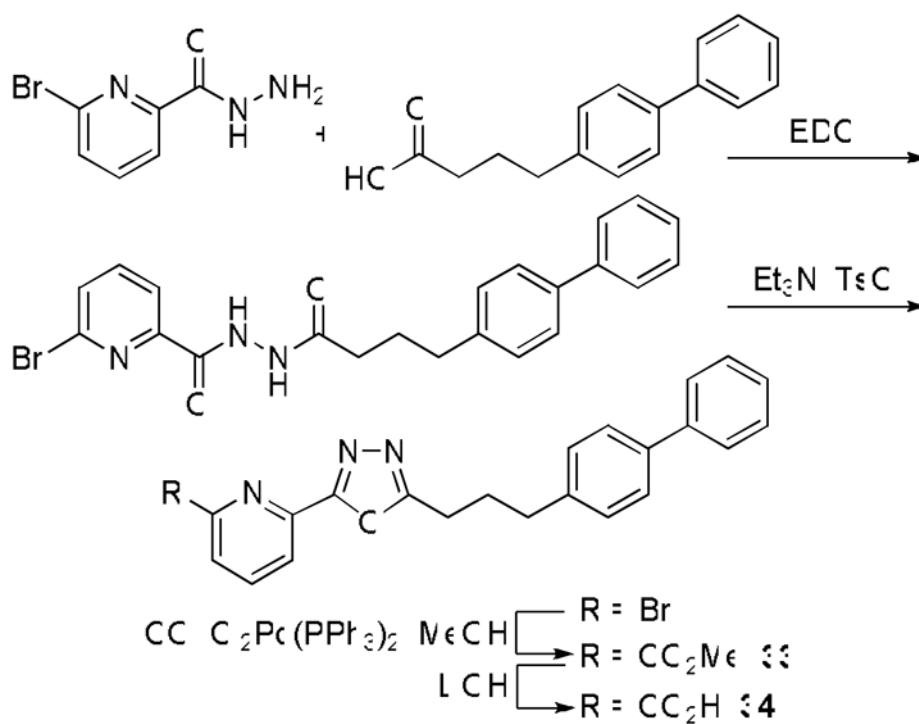


Scheme 6.

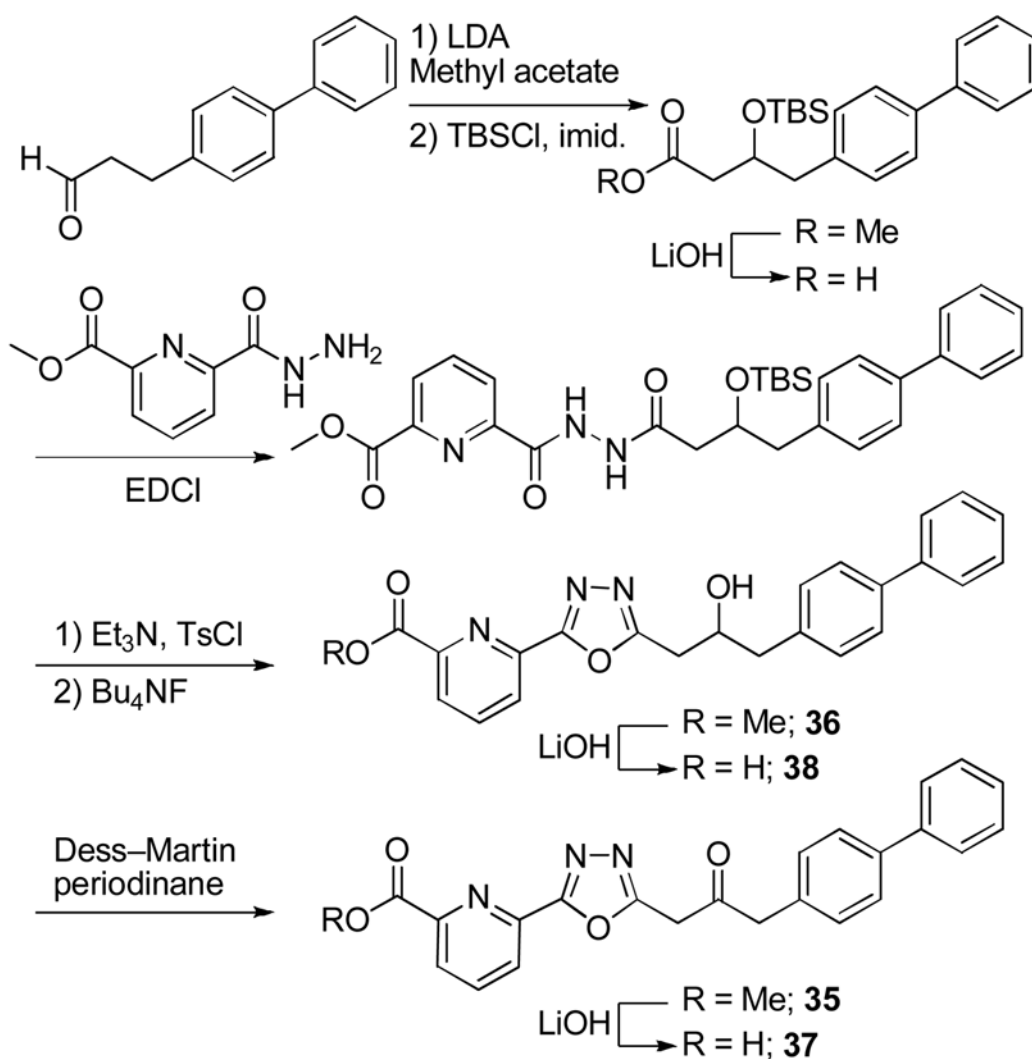




Scheme 7.



Scheme 8.



Scheme 9.